universität wien

DIPLOMARBEIT / DIPLOMA THESIS

Titel der Diplomarbeit / Title of the Diploma Thesis

„Characterisation of specific antibodies against different subunits of the neuronal nicotinic acetylcholine receptor (nAChR)“

verfasst von / submitted by

Rica Schadl

angestrebter akademischer Grad / in partial fulfilment of the requirements for the degree of

Magistra der Pharmazie (Mag.pharm.)

Wien, 2021/ Vienna, 2021

Studienkennzahl lt. Studienblatt / degree programme code as it appears on the student record sheet:	UA 449
Studienrichtung lt. Studienblatt / degree programme as it appears on the student record sheet:	Diplomstudium Pharmazie
Betreut von / Supervisor:	Assoc. Prof. Priv. Doz. Mag. Dr. Petra Scholze

Declaration

This work was realised at the Center for Brain Research, Medical University of Vienna under the supervision of Assoc. Prof. Priv. Doz. Mag. Dr. Petra Scholze.

I, Rica Schadl, declare that this thesis, entitled „Characterisation of specific antibodies against different subunits of the neuronal nicotinic acetylcholine receptor (nAChR)“, was written by me without any unauthorized help. No other sources than those cited and listed have been used.

_____ _____

Place, Date Signature

Acknowledgement

This thesis is the last step of a long journey with many ups and downs. I am very thankful for all the experience I have gained and all the lections I have learned throughout the last years. I would like to thank all my companions on my way, without whom this thesis would never have been written.

First of all, I want to thank my supervisor Petra Scholze for the opportunity to be part of her team and to realise this thesis in her laboratory, for her support and for sharing her expertise and knowledge with me. Additionally, I want to thank Friederike Steudle for introducing me to all the lab work and guiding me through my experiments.

A huge thank you belongs to my fellow students, who have become some of my closest friends, for the countless hours spent together at the university and especially in the library, for the shared suffering and thus much more bearable study sessions. Of course, I would like to thank them as well for the many unforgettable evenings, trips and moments during the last years.

Last but not least a special thanks goes to my whole family, especially my parents, sister and grandparents who always supported me no matter what. The same goes for my best friend. Even though they mostly didn't understand much about the subject, they always had an open ear for my worries and problems and built me up again.

Table of Contents

Abbreviations

2bp	two base pairs
aa	amino acids
ACh	Acetylcholine
APS	Ammonium persulfate
CNS	central nervous system
DNA	desoxyribonucleic acid
ER	Endoplasmic reticulum
GFP	Green fluorescent protein
HeBS	Hepes buffered saline
HEK-293 cells	Human embryonic kidney cells 293
HRP	Horseradish peroxidase
ICC	Immunocytochemistry
IgG	Immunoglobulin G
KLD	Kinase, ligase and DpnI
KO	Knockout
LB medium	Lysogeny broth medium
mAChR	Muscarinic acetylcholine receptor
mRNA	Messenger ribonucleic acid
nAChR	Nicotinic acetylcholine receptor
PBS	Phosphate buffered saline
PCR	Polymerase chain reaction
PVDF membrane	Polyvinylidene fluoride membrane
RIC-3	resistant to inhibitors of cholinesterase-3
RT	Room temperature
SDS	Sodium dodecyl sulfate
TE buffer	Buffer containing Tris and EDTA
TG	Tris glycine
TSS	Transformation and storage solution
WT	Wild type
α-BGT	α-bungarotoxin

Abstract

The neuronal nicotinic acetylcholine receptor (nAChR) is a ligand-gated ion channel formed by different α and β subunits and plays a key role in the central and peripheral nervous system. The composition of the subunits is crucial for the biophysical and pharmacological properties of the receptor but is also partly responsible for some pathogenesis. Subunit-specific antibodies are an important tool for further investigation of individual subunits and their composition in receptors. These antibodies must be suitable for the chosen methods and must therefore be sufficiently characterised and analysed beforehand. In this work, established as well as newly generated antibodies were tested for their suitability in future experiments.

In particular, this work focuses on the one hand on already existing antibodies against the α3, α4, β2 and β4 subunits, which form the heteropentameric α3β4 and α4β2 receptors, among others. These have already been tested and used in the past for the analysis of the corresponding subunits. Since the antibodies were gained from rabbits immunised with fusion proteins containing DNA fragments of the sequences of mouse subunits, they have so far only been used on murine tissue and transfected HEK-293 cells. The question that has now arisen is whether they recognize the human subunits and are suitable for methods to study human receptors as well.

All antibodies were analysed in native tissue of mice (habenula) and transfected HEK-293 cells by Western blot and selected antibodies were further analysed by immunocytochemistry (ICC) with transfected HEK cells.

The main part of this work is focused on the characterisation of newly generated antibodies directed against the human homopentameric α7 receptor. This receptor is of particular interest because the gene encoding for it, which is called CHRNA7, has been duplicated during human evolution. These duplicates, named CHRFAM7A and CHRFAM7AΔ2bp, are thought to be partly responsible for various diseases such as schizophrenia, Alzheimer's disease or epilepsy. The antibodies against these receptor subunits were also produced by previously immunised rabbits and characterised using the same methods.

Regarding the first question, the comparison of human and mouse DNA sequences showed that those of the α3 and β2 subunits show a high rate of similarity, whereas the sequences of the α4 and β4 subunits show greater differences. Therefore, it was assumed that the existing anti-α4 and -β4 antibodies would not recognize the human receptor subunits, while the ones against the α3 and β2 subunit could most likely be used to detect both, rodent and human

proteins. This hypothesis was confirmed in western blot as well as for the antibodies α3S1 and β2S19 in ICC.

The newly produced α7LS3 antibody gave promising first results in western blot and ICC, but needs to be further examined. All other antibodies of this generation gave no or only unspecific results in this work.

Zusammenfassung

Der neuronale nikotinische Acetylcholinrezeptor (nAChR) ist ein ligandengesteuerter Ionenkanal, der aus verschiedenen α- und β-Untereinheiten geformt wird und eine Schlüsselrolle im zentralen sowie peripheren Nervensystem spielt. Die Zusammensetzung der Untereinheiten ist dabei maßgeblich für die biophysikalischen und pharmakologischen Eigenschaften des Rezeptors, aber auch mitverantwortlich für verschiedene Pathogenesen. Um einzelne Untereinheiten und deren Zusammensetzung in den Rezeptoren näher untersuchen zu können, sind untereinheitenspezifische Antikörper ein wichtiges Werkzeug. Diese Antikörper müssen für die gewählten Methoden geeignet sein und daher zuvor ausreichend charakterisiert und analysiert werden. In dieser Arbeit wurden nun bereits etablierte, sowie neu generierte Antikörper auf die Eignung für die Verwendung bei zukünftigen Experimenten getestet.

Im speziellen fokussiert sich diese Arbeit einerseits auf bereits vorhandene Antikörper gegen die α3, α4, β2 und β4 Untereinheiten, die unter anderem die heteropentameren α3β4 und α4β2 Rezeptoren bilden. Diese wurden in der Vergangenheit bereits zur Analyse der entsprechenden Untereinheiten getestet und verwendet. Da die Antikörper von Kaninchen gewonnen wurden, die mit Fusionsproteinen, die DNA-Fragmente der Sequenzen der Untereinheiten der Maus enthalten, immunisiert wurden, wurden diese bisher nur an murinem Gewebe und transfizierten HEK-293 Zellen eingesetzt. Die Frage, die sich bezüglich dieser Antikörper nun stellte, ist, ob diese auch die humanen Untereinheiten erkennen und für Methoden zur näheren Erforschung der humanen Rezeptoren geeignet sind.

Alle Antikörper wurden im nativen Gewebe von Mäusen (Habenula) und transfizierten HEK-293 Zellen mittels Western Blot und ausgewählte Antikörper auch mittels immunozytochemischer Färbungen von transfizierten HEK-Zellen analysiert.

Der Hauptteil der Arbeit befasst sich aber mit der Charakterisierung von neu generierten Antikörpern, die gegen den humanen homopentameren α7 Rezeptor gerichtet sind. Dieser Rezeptor ist von besonderem Interesse, da im Laufe der Evolution des Menschen das für diesen kodierende Gen CHRNA7 dupliziert wurde und die Duplikate CHRFAM7A und CHRFAM7AΔ2bp für die Entstehung diverser Krankheiten wie Schizophrenie, Morbus Alzheimer oder Epilepsie, mitverantwortlich gemacht werden. Diese Antikörper wurden ebenfalls durch zuvor immunisierte Kaninchen produziert und mit Hilfe derselben Methodik charakterisiert.

Bezüglich der ersten Frage ergab der Vergleich der DNA-Sequenzen von Mensch und Maus, dass die der α3 und β2 Untereinheiten einen hohen Ähnlichkeitsgrad aufweisen, die Sequenzen der α4 und β4 Untereinheit weisen im Gegensatz dazu größere Unterschiede auf. Daher wurde angenommen, dass die bereits vorhandenen anti-α4 und -β4 Antikörper die humanen Rezeptoruntereinheiten nicht erkennen werden, während die anderen Antikörper mit hoher Wahrscheinlichkeit zur Detektion beider Proteine verwendet werden könnten. Diese Annahme wurde sowohl im Western Blot als auch für die zwei Antikörper α3S1 und β2S19 in der Immunozytochemie (ICC) bestätigt.

Der neu hergestellte α7LS3 Antikörper gab sowohl im Western Blot als auch in der ICC vielversprechende erste Ergebnisse, muss aber noch weiter untersucht werden. Alle anderen Antikörper dieser Generation lieferten im Rahmen dieser Arbeit keine oder nur unspezifische Ergebnisse.

1 Introduction

1.1 The cholinergic system

Nicotinic acetylcholine receptors (nAChRs) play a key role in the cholinergic system. Acetylcholine (ACh) is synthesised, stored and released by cholinergic neurons and is involved in various cognitive processes and movement control through the activation of nAChRs. This phylogenetically very old pathway is important for physiological functions like sleep, anxiety, addiction, fatigue, pain [1–3]. Moreover, dysfunction caused by decline, disruption or alterations in nAChRs are linked to diseases such as epilepsy, schizophrenia, Parkinson's disease or Alzheimer's disease. [4]

Beside the nicotinic receptor, there is another receptor subtype activated by the endogenous neurotransmitter acetylcholine, the metabotropic muscarinic acetylcholine receptor (mAChR). This receptor is named after the toxin muscarine which is an exogenous activator of the receptor. The nicotinic receptor is activated by the alkaloid nicotine in micro- to submicroseconds while the activation of the metabotropic receptors takes milliseconds to seconds. Another major difference between the subtypes is, that the mAChRs belong to the group of G protein-coupled receptors while the ionotropic nicotinic receptors are ligand-gated ion channels. Both receptors are expressed in the central nervous system (CNS) as well as in the peripheral nervous system (PNS) and can be found in non-neuronal tissue as well [2,5].

The family of nAChRs is further divided into two different subtypes. There are muscle specific and neuronal specific receptors [3]. However, this work focuses on the neuronal nicotinic acetylcholine receptor only, which is described in detail below.

1.1 Structure and function of the neuronal nicotinic acetylcholine receptors (nAChR)

Neuronal nicotinic acetylcholine receptors are transmembrane proteins consisting of 5 subunits arranged around the central water-filled pore which is permeable to the small monovalent Na^+ and K^+ ions and to the divalent Ca^{2+} ions [4,6,7]. So far, there are nine different alpha (α2-α10) and three different beta (β2-β4) subunits known. Therefore, many different compositions with up to 4 different subunits are possible. Heteromeric $\alpha\beta$ receptors can be formed with α2-α4 and all of the beta subunits, α7-α9 can build homomeric nAChRs and α10 is capable to form a heteromer with α9 [4]. In the CNS, the main subunits are α4, α7 and β2,

while $\alpha 3$ and $\beta 4$ are predominant in the periphery [6]. Each of the subunits consists of approximately 500 to 600 amino acids (aa). Moreover, as nAChRs belong to the superfamily of the so-called “Cys-loop” receptors, they are composed of different typical domains. First, there is the huge extracellular N-terminus which is about 200 aa long, hydrophilic and carries the binding site for acetylcholine [6,8,9]. Like all the other family members, nAChRs contain a high conserved disulfide bond between two cysteines, the Cys-loop, which is crucial for agonist binding [2,10]. After four hydrophobic transmembrane domains (M1-M4) of about 20 aa each, linked through alternating intracellular and extracellular loops, the short extracellular C-terminus is following. The cytoplasmic loop between M3 and M4 is the largest and variable in size and sequence. The structure of the receptor is schematically illustrated in Figure 1.1 [2,6,8,9].

The ionic pore is built mainly by the M2 helices which are directed towards the pore lumen and are responsible for the ion selectivity control [10,12]. The “charge selectivity filter” is indicated as a structural equivalent region in all LGICs in the intracellular border of the M2 domain. Not only charged residues and the electrostatics of them, but also the size of the minimum pore diameter of the channel is relevant for ion-selectivity [6,13].

The binding site for acetylcholine is located at the interface between the subunits which means either between the α and the β subunit for heteromeric receptors or on each interface between subunits of homomeric receptors. Therefore, $\alpha\beta$ receptors have only two binding sites, while homomeric nAChRs have five binding sites, as shown in part c of the Figure 1.1 [14,15].

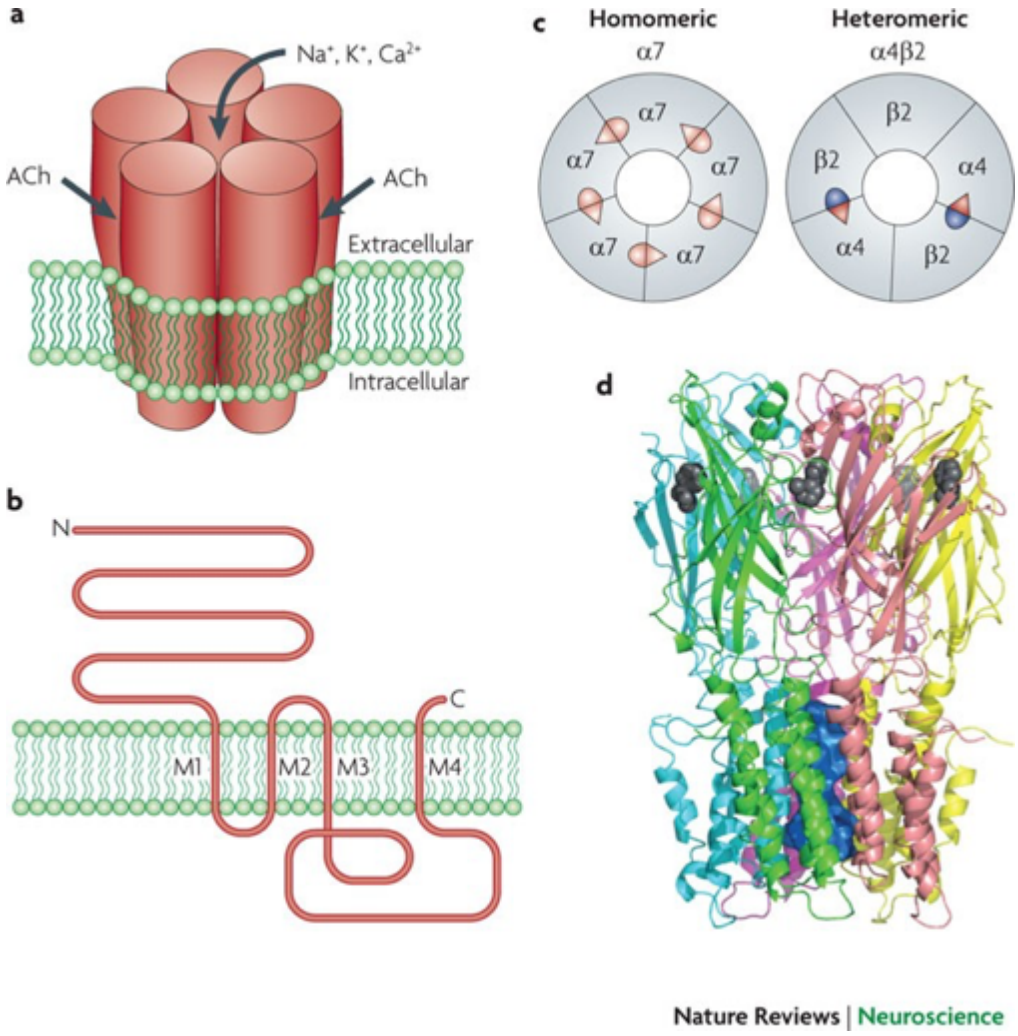

Figure 1.1*: Structure of nAChRs* [11].
a. nAChRs are formed by five subunits arranged around a central pore. b. All of these subunits are consisting of the same parts: the huge extracellular N-terminus, four hydrophobic transmembrane domains (M1-M4), a large intracellular loop between M3 and M4 and a short extracellular C-terminus. c. The subunits are forming homomeric or heteromeric nAChRs. Schematic illustration of the most common types in brain, $\alpha 7$ and $\alpha 4\beta 2$, including the binding sites. d. Nicotine molecules (grey) presented in the binding pockets of an $\alpha 7$ homopentamer model. The ion channel is shown in dark blue.

1.2 α3β4 and α4β2 receptors

The $\alpha 3\beta 4$ receptors are predominant in the peripheral nervous system and are expressed at high levels in the pineal gland or autonomic ganglia and also in subsets of neurons in the medial habenula or interpeduncular nucleus [16,17]. On the other hand, $\alpha 4$ and $\beta 2$ are present in the central nervous system and account for 90% of the high affinity neuronal receptors for nicotine in mammalian brain [18].

Furthermore, the $\alpha 4\beta 2$ receptor was the first receptor subtype characterised in rat brain. This subtype binds the most common nicotinic agonists with high affinity and knocking down one of its subunits leads to a loss of the high affinity binding in most brain regions [14,16]. A chronic

exposure of nicotine is claimed to be responsible for an up-regulation of the number of $\alpha 4\beta 2$ receptors in rodent and human brain. This effect was observed in post-mortem brains of human smokers [17,19], whereas a selective reduction of these receptors in the cortex is linked to Alzheimer's disease [17,19,20].

Studies about the $\alpha 3\beta 4$ subtype showed that it is involved in noradrenaline release in the hippocampus and it is also supposed to be an autoreceptor in the neurons of the habenulo-interpeduncular pathway [17]. $\alpha 3$ knockout (KO) mice revealed that this subunit is essential for survival, as it is a critical part of fast synaptic transmission in the autonomic nervous system [16,21].

1.3 The α7-subunit and the duplication of the gene CHRNA7

$\alpha 7$ receptors can be found throughout the brain with the highest levels of expression in hippocampus and cortex [22], but can also be found in the periphery like on macrophages [23].

They are suggested to be the main binding proteins for α-bungarotoxin (α-BGT) in the rodent brain. A study with knockout mice showed that $\alpha 7$ is required for the high affinity α-BGT binding sites, as there was no significant α-BGT binding in $\alpha 7$-deficient mice [24]. These receptors account for 90% of the α-BGT sensitive receptors with high affinity in the mammalian brain [18].

The combination of subunits in heteropentameric receptors also provides a large variability of pharmacological characteristics and kinetics of activation and desensitization. While the receptor subtypes mentioned before are characterised through a slow desensitization rate, the homopentameric $\alpha 7$ receptor undergoes a fast activation and desensitization. All of the described subtypes have an active state with low to medium ($\alpha 4\beta 2$) affinity for ACh in common [25].

The gene encoding for the $\alpha 7$ neuronal nicotinic receptor (CHRNA7) is located on chromosome 15q14, but structurally differently organised and with a different number of introns and splicing sites compared to the genes of the other subunits [26]. Mutations in this gene, leading to decreased expression and function of the receptor, are linked to diseases like schizophrenia. One of the first evidences of a linkage between the auditory sensory deficit in patients with schizophrenia and a polymorphism at the gene for the $\alpha 7$ receptor gene on chromosome 15q13-14 was shown in a study in 1997 [27]. Soon a partial duplication of the

gene was found proximal to the full length CHRNA7 [28] and suggested to be responsible for the reduced functionality of the $\alpha 7$ receptor, when expressed [29]. Several other studies support this hypothesis [30]. Since this duplication of the gene occurred about 1 million years ago and it is assumed that chimpanzee and human lineage diverged about 6 million years ago, the mutation is only found in human. Consequently, it cannot be found in rodents [31].

1.3.1 Partial duplication of CHRNA7 on chromosome 15

Prior to the already mentioned duplication of the gene encoding for $\alpha 7$, exons of the unc-51 like kinase 4 gene (numbered with A, B, C and E) located at chromosome 3 were duplicated on chromosome 15. In combination with some exons (numbered with D, F and G) duplicated from other regions of chromosome 15, the genetic element FAM7A (A-F) was built. There are at least four copies of these exons on chromosome 15, arranged around CHRNA7 which can be seen in part A of Figure 1.2 [32]. The human gene for the $\alpha 7$ subunits consists of 10 exons with at least 75 kb [28]. Following, exons 5-10 were duplicated along with the desoxyribonucleic acid (DNA) of the third copy of FAM7A and inserted 1.6 Mb upstream, interrupting the first copy of FAM7A. This duplication is termed CHRFAM7A and it has a reverse orientation which means tail to head with the original gene, shown in part B of Figure 1.2 [28,32,33].

In some humans, another mutation in the duplicated gene followed. A deletion of two base pairs (2bp) in exon 6 of CHRFAM7A was found, leading to an inversion of the gene causing the same orientation as the full-length gene, as presented in panel C of Figure 1.2. This gene is termed CHRFAM7AΔ2bp [28,34,35].

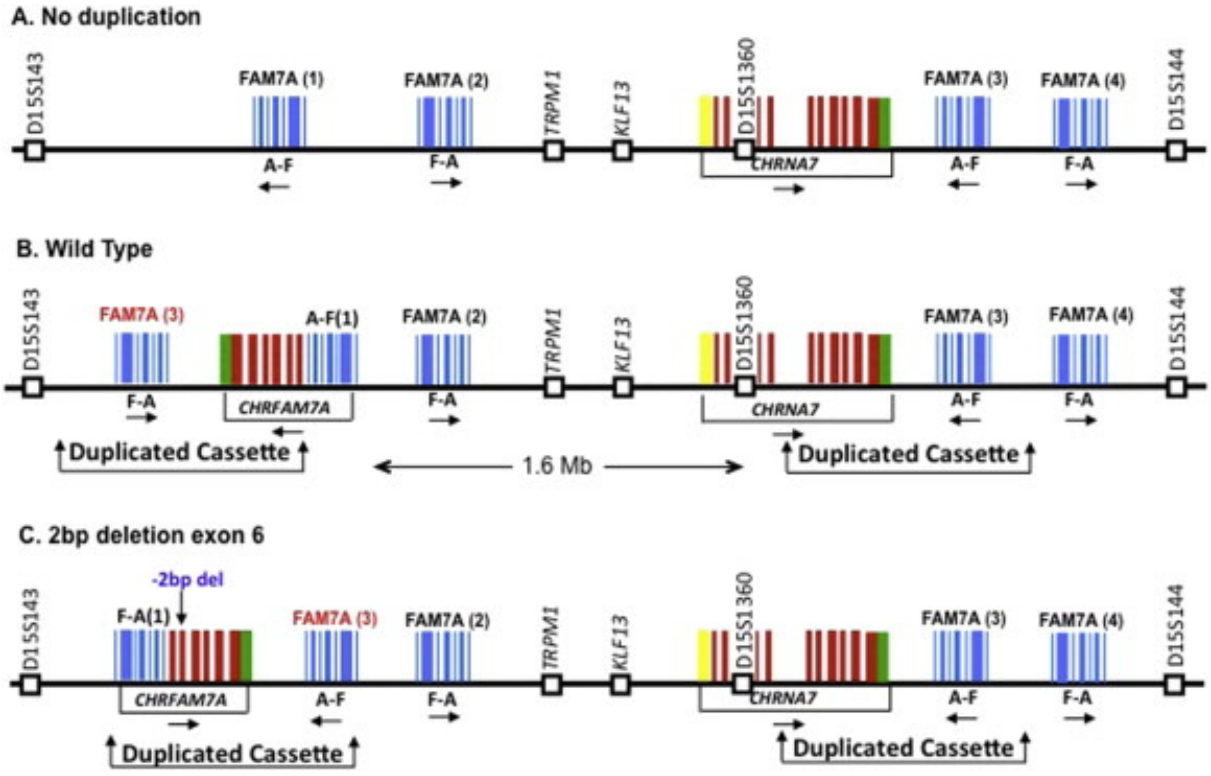

***Figure 1.2**: Duplication of the CHRNA7 gene* [32].
A. Several exons were duplicated from chromosome 3 and other regions of chromosome 15, forming FAM7A. There are at least four copies of FAM7A at chromosome 15, near CHRNA7. B. Exons 5-10 of CHRNA7 were duplicated along with FAM7A (3) and inserted 1.6 Mb upstream, forming CHRMFAM7A. This duplication interrupts FAM7A (1) and has reverse orientation. C. Another mutation within CHRFAM7A is a deletion of 2bp in exon 6, leading to an inversion of the gene, forming CHRFAM7AΔ2bp.

1.3.2 Translation products of CHRNA7, CHRFAM7A and CHRFAM7AΔ2bp and their topology

The products of translation of the genes CHRFAM7A and CHRFAM7AΔ2bp are presented in Figure 1.3 and the putative topology of α7, dupα7 and dupΔα7 is shown in Figure 1.4. The translation of wild type CHRFAM7A starts with an initiation methionine in exon B and the product contains a part of exon B and exon A from the FAM7A gene as well as exons 5-10 of CHRNA7. This gene product is named dupα7 and lacks the signal peptide, a glycosylation site and part of the agonist binding site.

If the translation of CHRFAM7AΔ2bp is started with the same start codon in exon B, a truncated peptide will be produced because of a frameshift caused through the 2bp deletion, leading to a stop codon. However, in exon 6 two additional start codons are present, playing a key role in the translation of CHRFAM7AΔ2bp. Translation starting at one of those start codons leads to a peptide that is out of frame for 6 or 13 amino acids, depending on the start codon used. Nevertheless, after a shift of the reading frame through the 2bp deletion, all of

the other amino acids are translated correctly like the original α7. The translation product of CHRFAM7AΔ2bp is named dupΔα7, is smaller than the α7 subunit and dupα7 and lacks the signal peptide as well as nearly the entire binding site for ACh. Like dupα7, it misses a glycosylation site, but in addition also the cysteine bridge, which is retained in dupα7 [31], [35], [36].

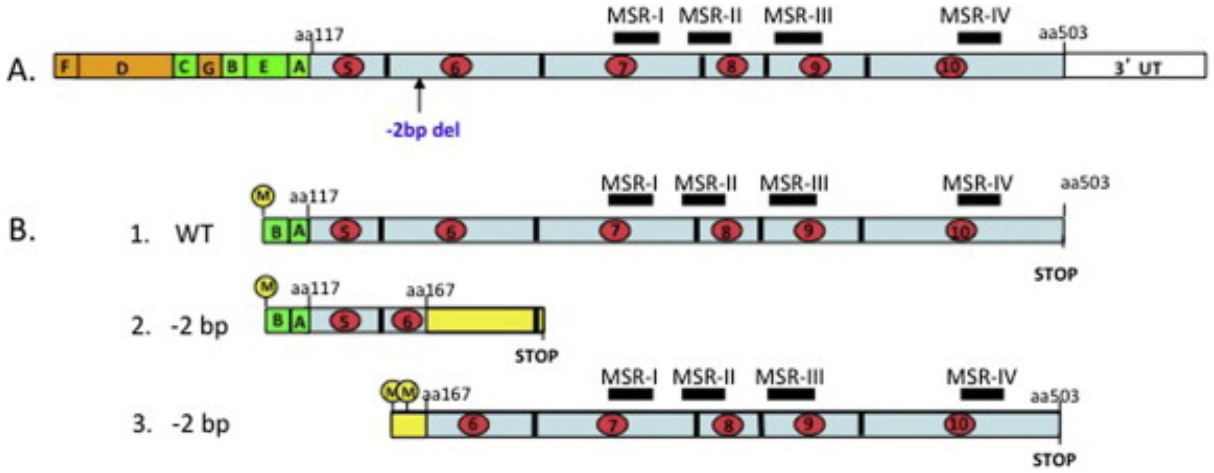

Figure 1.3: *Translation products of CHFAM7A and CHRFAM7AΔ2bp* [32].
A. mRNA of CHRFAM7A. B.1 The translation of wild type CHRFAM7A starts in exon B and the product contains part of exon B and exon A of FAM7A and exons 5-10 of CHRNA7. B.2 If the 2bp deletion is present, a translation, starting in exon B, leads to a stop codon in exon 6 and a truncated peptide. B.3 If the translation of CHRFAM7AΔ2bp starts with an initiation methionine in exon 6, some amino acids are out of frame, but the sequence reverts to the original one of α7 after the 2bp deletion.

The CHRFAM7A gene is widely expressed in the mammalian brain, like the full-length α7 gene, although at very low levels [36]. The duplicated subunits dupα7 and dupΔα7 are assembled with the α7 subunit, transported and integrated into the cell membrane as shown in part D of Figure 1.4. If only one truncated subunit is assembled into the receptor, already two binding sites for acetylcholine are eliminated [32]. All other, further truncated products produced through translation starting at other ATGs in the messenger ribonucleic acid (mRNA) of CHRFAM7A, are unlikely to assemble with the full-length subunit [36]. Apparently, the truncated peptides do not assemble alone [37]. When assembled with α7, dupα7 is suggested to be a dominant negative regulator of the receptor activity and function by reducing the functional α7 nAChRs, as studies with oocytes showed. The function is further decreased when the α7 subunit is co-expressed with dupΔα7. The mechanism of how the function is impacted

by the truncated is not totally understood yet, though [29,37]. Newer studies showed evidence that CHRFAM7A decreases the binding of a ligand to the α7 nAChR in vivo [38].

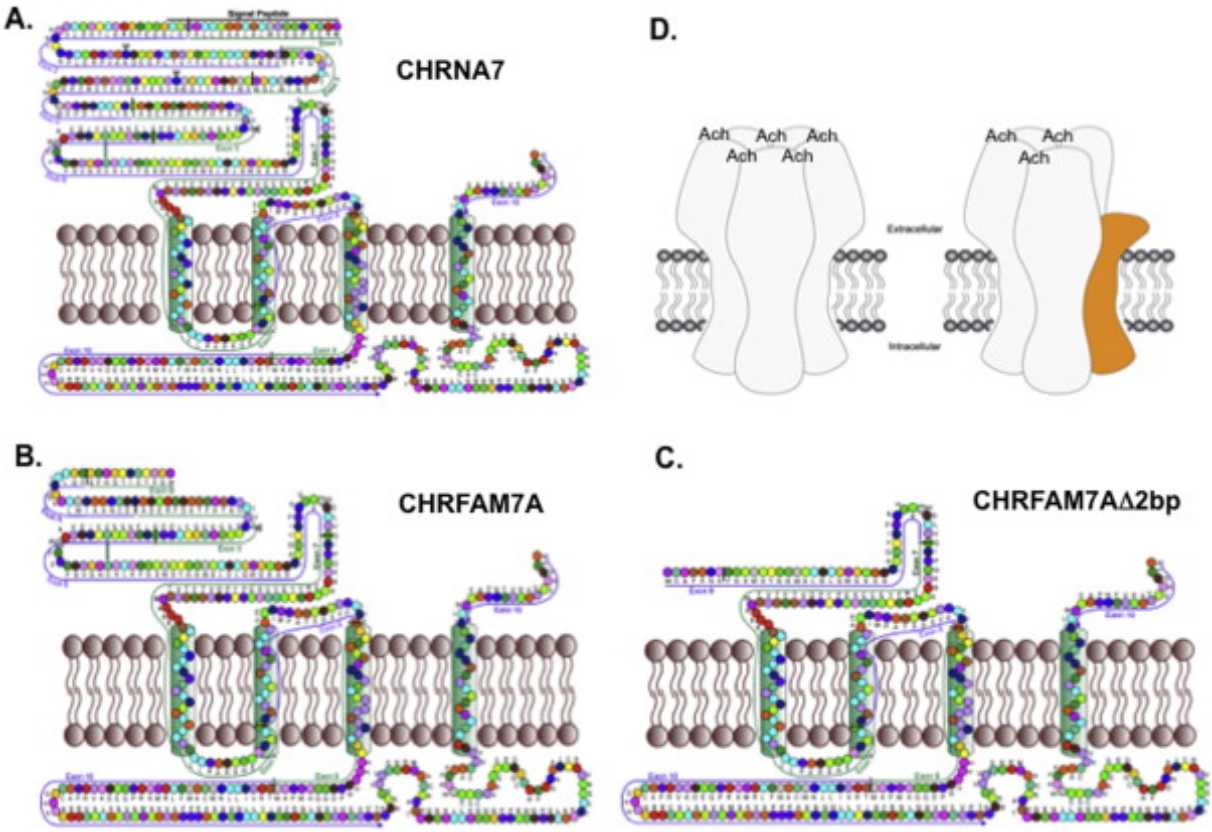

Figure 1.4: *Topology of CHRNA7, CHRFAM7A and CHRFAM7AΔ2bp gene products* [32].
A. The full-length α7 subunit has a huge N-terminus containing a signal peptide, three glycosylation sites, a cysteine bridge and the binding site for ACh. B. The gene product of CHRFAM7A is missing the signal peptide and a glycosylation site, as well as a part of the binding site. C. The gene product of CHRFAM7AΔ2bp additionally lacks the cysteine bridge and nearly the entire binding site. D. On the left site a normal pentameric α7 nAChR is shown. On the right site a α7 nAChR containing one truncated subunit (orange) is shown. If assembled, these receptors are missing two binding sites for acetylcholine.

1.4 Role of the chaperones NACHO and RIC-3

The chaperons NACHO and resistant to inhibitors of cholinesterase (RIC)-3 play an essential role in expression, folding and function, assembly, transportation and membrane insertion of α7 nAChRs [39–41]. It was found that a knockout of NACHO is connected to a loss of α-BGT binding sites, which means there are no functional α7 receptors present on the cell surface. Therefore, this protein is able to regulate or enhance maturation, folding, assembly, membrane insertion and consequently, function of α7 [41]. Further, NACHO is not only required for binding of α-BGT at α7 neurons, but also alters the binding of [^{3}H]epibatidine to some other nAChRs [42]. Binding of epibatidine indicates a correct receptor assembly as its

binding site lies at the interface between the subunits [43]. A study with transfected human embryonic kidney (HEK) cells showed that $\alpha 7$ and $\alpha 3\beta 2$ nAChRs only bind [^{3}H]epibatidine when co-transfected with NACHO. The binding to $\alpha 4\beta 2$ and $\alpha 3\beta 4$ receptors is not depended on the presence of NACHO, but a co-transfection enhanced the signal clearly. Therefore, NACHO mediates assembly and function of different nAChRs in the mammalian brain [42].

The second chaperon RIC-3 is a protein first identified in *Caenorhabditis elegans* [44]. It is a transmembrane protein found inside the cell, apparently predominantly in the endoplasmic reticulum (ER), and expressed in muscle and nerve cells [40]. RIC-3 belongs to a conserved gene family and effects the maturation of the $\alpha 7$ nAChR [39]. An experiment with oocytes showed, that the number of receptors in total is increased by RIC-3, as well as the number that reaches the cell surface [45].

RIC-3 synergises with NACHO as it is not essentially required for the functionality of $\alpha 7$ but enhances the effects of NACHO, whole-cell patch-clamp recordings showed. Other experiments showed that RIC-3 requires NACHO for its effects on α-BGT and [^{3}H]epibatidine binding. Thus, an evidence that NACHO initially mediates early steps of receptor maturation is given [42].

1.5 Antibody generation and characterisation

Because of the already mentioned cognitive processes and diseases different nAChR subunits are being involved in, there is the need for specific antibodies against the different subunits for further examination of the correlations between the subunits and pathologies.

Antibodies can be generated by immunisation of rabbits with fusion proteins. These proteins contain the target sequence of the subunit, which is linked to a maltose-binding protein (MBP). Then, the sera of the immunised rabbits can be purified via affinity chromatography to isolate the antibodies [46,47].

An aspect that needs to be mentioned here is that although quite a lot of information about the mRNA levels of the subunits can be found in literature, these are not always identical to the protein levels. Several studies have shown that mRNA expression often has low correspondence with protein expression. Also, environmental changes and the rates of protein degeneration can have an effect on the protein expression [48]. An increase or decrease in the protein levels of certain nAChR subunits, such as the $\alpha 7$ subunit, is not accompanied by a change in mRNA levels. This is the result of a publication that investigated

this relation of mRNA and protein levels in the brains of smokers and patients with Alzheimer's disease, also suggesting that post-transcriptional regulations can modify protein expression [49].

Although there is already quite some information about the mRNA [50], especially for the dup$\Delta\alpha$7 receptor protein not much is known about protein expression.

Studies have shown, why the characterisation of new antibodies is so important: In these studies commercially available antibodies were tested with different methods and appeared to be not useful for some techniques [51] and in the other study α7 antibodies were validated with different strategies, leading to the same result [52]. Since no suitable antibodies against the α7 subunit and its duplications were available at the time of this work, new antibodies were previously generated by our group. These were gained from immunised rabbits as described in Mossier *et al.* [46] and mentioned above.

1.6 Aim of this study

This study focuses on answering two main questions:

a. Do antibodies against the α3, α4, β2 and β4 subunits, gained from rabbits immunised with fusion proteins containing DNA fragments from mice nAChR subunits, also recognise the human proteins?

b. Do the newly generated antibodies against the human α7 subunit and its duplication specifically recognise the proteins in western blot and immunocytochemistry?

Concerning the first question, the already established antibodies α3S1, α4S26, β2S19, β4S4-S6 and β4S22 were tested and further investigated with western blot. The ones which were able to detect the human subunits were further analysed with immunocytochemistry. Additionally, the suitability for experiments with the subunits from rats was also tested and compared.

The antibodies α7N S1 and S2, α7L S3 and S4, dupα7N S5 and S6 and 2bpα7N S7 and S8 were purified from immunised rabbits and the question was if they recognize specifically the corresponding subunit in western blot and immunocytochemistry. In a future project they are

meant to be used to further investigate the $\alpha 7$ receptor and its duplication in human iPSC-derived neurons. Therefore, they need to be sufficiently characterised and analysed before. Since these antibodies were generated against the DNA sequence of human subunits, it was also interesting to see, if the receptor could be detected in native tissue from mice and rats.

2 Materials

All reagents and materials used in this work were purchased from Merck KGaA, Sigma-Aldrich Inc., Thermo Fisher Scientific Inc., Carl Roth GmbH + Co. KG, VWR International and Bio-Rad Laboratories Inc., if not otherwise mentioned.

2.1 Mutagenesis and cloning

***Table 2.1**: Primers for mutagenesis including name, sequence and the annealing temperature.*

Name	**Sequence**	**Annealing Temp.**
b2flag2-Q5-FW	tgacaaggctgcagccGAGGAGCGGCTGGTGGAG	68 °C
b2flag2-Q5-RV	tcgtcatccttgtaatcTGTATCCGTACCCCACACC	
b4flag2-Q5-FW	tgacaaggccggatccAATGCGGAGGAAAAGCTGATGGACG	72°C
b4flag2-Q5-RV	tcgtcatccttgtaatcGGCCACGCGGCAGTTCCC	
a3myc2-Q5-FW	ggaggacctggcaggatccTTTGAGCGGCTGTTTGAAG	64 °C
a3myc2-Q5-RV	tcggagatcagcttctgctcTAGACGGTGCTCAGCCTC	
a4myc2-Q5-FW	ggaggacctggcaggatccACCCGGGCCCACGCCGAG	72 °C
a4myc2-Q5-RV	tcggagatcagcttctgctcCTCCACATGGCTGCTGGCGCG	
a5his2-G5-FW	tcacgccggatccCTAGCGGGCGCGGCGGGC	72 °C
a5his2-G5-RV	tggtgatggtgatgACCGCSGCGCCCCGCGAC	
a7myc2-Q5-FW	ggaggacctggccggatccCAGAGGAAGCTTTACAAGGAG	64 °C
a7myc2-Q5-RV	tcggagatcagcttctgctcGAACTCGCCTTGCAGGGA	
delta2bp_ Q5_His2_FW	tcacgccggatccTACGCTGGTTTCCCTTTG	63 °C
delta2bp_ Q5_His2_RV	tggtgatggtgatgCATCTCGAGGCTAGCCTA	
FAM-Flag2-FW	AGCCTCGAGATGGATTACAAGGATGAC GATGACAAGGCAGGATCCCAAAAATATTGCATCTACCAG	58 °C
FAM-MluI-RV	CAGATCACGCGTTTACGCAAAGTCTTTGGACACGGC	

***Table 2.2**: 1% Agarose gel*

Agarose	1 g
TE buffer	up to 100 ml
GelRed®	5 µl

Table 2.3: *TE buffer pH=8.0*

Tris	10 mM
EDTA	1 mM

The TE buffer was sterilised by autoclaving at 121°C before use.

Table 2.4: *TSS pH=6.5*

Trypton/Pepton	0.25 g
Yeast Extract	0.125 g
NaCl / 2M NaCl	0.146 g / 1.25 ml
PEG 3000/3350	2.5 g
DMSO	1.25 ml
MgCl2 ml 1M	1.25 g
dH_2O	up to 25 ml

Table 2.5: *LB-Medium pH=7.0*

Trypton/Pepton	20 g
Yeast Extract	10 g
NaCl	20g
dH_2O	up to 2000 ml
Optional: ampicillin (100 mg/ml)	100 µg/ml
Optional: tetracycline (10 mg/ml)	10 µg/ml

The LB-medium was sterilised by autoclaving at 121°C before use. Afterwards, antibiotic was added, if needed. For LB-plates 7.5 g agar-agar was added to 500 ml medium, after autoclaving it was cooled down to 55 °C and antibiotic was added, before pouring into 10 cm dishes.

2.2 HEK cells cultivation and transfection

Table 2.6: *HEK complete medium*

DMEM (+) GlutaMax™ (Gibco®)	500ml
Fetal Bovine Serum	50ml
Pen Strep (Gibco®)-100x (Penicillin 10 000 U/ml Streptomycin 10 mg/ml)	5ml
MEM (non-essential amino acids) (Gibco®)	5ml

Table 2.7: *HeBS buffer pH=7.11*

Hepes	2.9 g
NaCl	4.1 g
$Na_2HPO_4*2H_2O$	67 mg
dH_2O	up to 250 ml

Table 2.8: *1x PBS buffer pH=7.3*

KCl	200 mg
KH_2PO_4	200 mg
NaCl	8 g
$Na_2HPO_4*2H_2O$	766 mg
dH_2O	up to 1000 ml

2.3 Membrane preparation

Table 2.9*: Homogenisation buffer*

Hepes 100mM pH=7.5	5 ml
EDTA 500mM pH=8	100 µl
Sucrose	5.1 g
dH_2O	up to 50 ml
cOmplete™ Protease inhibitor cocktail tablet (F. Hoffmann-La Roche AG)	40 mg

Table 2.10: *Washing buffer*

Hepes 100mM pH=7.5	5 ml
EDTA 500mM pH=8	100 µl
dH_2O	up to 50 ml
cOmplete™ Protease inhibitor cocktail tablet (F. Hoffmann-La Roche AG)	40 mg

2.4 Western blot

Table 2.11: *10% Tris-glycine separating gel (A) 5% Tris-glycine stacking gel (B)*

A

dH_2O	5.0 ml
Separation gel buffer (Table 2.12)	3.75 ml
Bis-Acrylamide	6.0 ml
10% SDS	150 µl
APS	150 µl
TEMED	15 µl

B

dH_2O	2.4 ml
Stacking gel buffer (Table 2.13)	1.2 ml
Bis-Acrylamide	850 µl
10% SDS	50 µl
APS	50 µl
TEMED	5 µl

Table 2.12: *4x Separation gel buffer pH=8.8*

Tris	18.15 g
dH_2O	up to 100 ml

Table 2.13: *4x Stacking gel buffer pH=6.8*

Tris	6.05 g
dH_2O	up to 100 ml

Table 2.14: *10x TG*

Tris	30 g
Glycine	144 g
dH_2O	up to 1000 ml

Table 2.15: *Running buffer*

10X TG	100 ml
10% SDS	10 ml
dH_2O	up to 1000 ml

Table 2.16: *Transfer buffer*

10X TG	100 ml
10% SDS	1 ml
Methanol	200 ml
dH_2O	up to 1000 ml

Table 2.17: *10x PBS pH=7.4*

Na_2HPO_4 x $2H_2O$	17.8 g
KH_2PO_4	2.4 g
KCl	2g
NaCl	80g
dH_2O	up to 1000 ml

Table 2.18: *5% Blocking buffer*

Low fat milk Powder	5 g
1x PBS	up to 100 ml
Tween 20	100 µl

Table 2.19: *1,5% Washing buffer*

Low fat milk Powder	15 g
1x PBS	up to 1000 ml
Tween 20	1 ml

Table 2.20: *4x SDS-Page Sample buffer*

Tris/HCl pH=6.8	12.5 ml
Glycerin	20 ml
β-Mercaptoethanol	10ml
SDS	4g
Pyronin Y	0,02g
dH_2O	up to 50 ml

Table 2.21: *Primary antibodies used in western blot*

Primary Antibody	**Concentration**	**Working concentration/ dilution**
anti-myc tag antibody clone 4A6, produced in mouse (Sigma-Aldrich®, 05-724)		1:2000
anti-flag tag antibody clone M2, produced in mouse (Sigma-Aldrich®, F9291)		1:2000
anti-his tag antibody (Abbexa Ltd, abx005576)		1:2000
α3 S1	205ng/µl	0,5µg/ml
α4 S26	410ng/µl	0,5µg/ml
β2 S19	434ng/µl	0,5µg/ml
β4 S4	302ng/µl	0,5µg/ml
β4 S5	140ng/µl	0,5µg/ml
β4 S6	551ng/µl	0,5µg/ml
β4 S22	504ng/µl	0,5µg/ml
α7N S1 §3/1 + §3/2	387ng/µl	0,5µg/ml
α7N S1 §3	343ng/µl	0,5µg/ml
α7N S2 §3	256ng/µl	0,5µg/ml
α7L S3 §3/1 + §3/2	564ng/µl	0,5µg/ml
α7L S3 §3	444ng/µl	0,5µg/ml
α7L S4 §3	260ng/µl	0,5µg/ml
dupα7N S5 §3	158ng/µl	0,5µg/ml
dupα7N S6 §3	181ng/µl	0,5µg/ml
2bpα7N S7 §3	198ng/µl	0,5µg/ml
2bpα7N S8 §3	210ng/µl	0,5µg/ml

Table 2.22: *Secondary antibodies used in western blot*

Secondary Antibody	**Working concentration/ dilution**
Peroxidase-conjugated IgG Fraction Monoclonal Mouse Anit-Rabbit IgG, light chain specific (Jackson ImmunoResearch Europe Ltd)	1:10000
Peroxidase-conjugated AffiniPure Goat Anti-Mouse IgG, light chain specific (Jackson ImmunoResearch Europe Ltd)	1:10000

Table 2.23: *Molecular weight marker*

Molecular weight marker	**Working concentration/ dilution**
Blue Plus® Protein Marker (14-100 kDa) (TransGen Biotech Co., Ltd, DM101)	1:6
Magic Mark™ XP Western Protein Standard (Invitrogen™, LC5602)	1:20 – 1:50

2.5 Immunocytochemistry (ICC)

Table 2.24: *Blocking Solution for ICC*

Bovine Serum Albumin	3g
Sodium Azide	0,3g
Normal Donkey Serum	1 ml
10% Triton X	1 ml
1x PBS	up to 100 ml

Table 2.25: *Dilution Solution for ICC*

Bovine Serum Albumin	3g
Sodium Azide	0,3g
Normal Donkey Serum	1 ml
Tween 20	1 ml
1x PBS	up to 100 ml

Table 2.26: *Primary antibodies used in ICC*

Primary Antibody	**Concentration**	**Working concentration/ dilution**
anti-myc tag antibody clone 4A6, produced in mouse (Sigma-Aldrich®, 05-724)		1:400
anti-flag tag antibody clone M2, produced in mouse (Sigma-Aldrich®, F9291)		1:400
anti-his tag antibody (Abbexa Ltd, abx005576)		1:400
penta his antibody (Qiagen® 34660)		1:400
his-probe antibody (H-15) (Santa Cruz Biotechnology®)		1:400
α3 S1	205ng/µl	0,4µg/ml
β2 S19	434ng/µl	0,4µg/ml
α7N S1 §3/1 + §3/2	387ng/µl	0,4µg/ml
α7N S1 §3	343ng/µl	0,4µg/ml
α7N S2 §3	256ng/µl	0,4µg/ml
α7L S3 §3/1 + §3/2	564ng/µl	0,4µg/ml
α7L S3 §3	444ng/µl	0,4µg/ml
α7L S4 §3	260ng/µl	0,4µg/ml
dupα7N S5 §3	158ng/µl	0,4µg/ml
dupα7N S6 §3	181ng/µl	0,4µg/ml
2bpα7N S7 §3	198ng/µl	0,4µg/ml
2bpα7N S8 §3	210ng/µl	0,4µg/ml

Table 2.27: *Secondary antibodies used in ICC*

Secondary Antibody	**Working concentration/ dilution**
Alexa Fluor® 488 donkey anti-rabbit IgG (Invitrogen™ A29206)	1:1000
Alexa Fluor® 568 donkey anti-mouse IgG (Invitrogen™ A10037)	1:1000

3 Methods

3.1 Amino acid alignments

To get an idea if the antibodies initially directed against mouse subunits would also recognise the human or rat proteins, the amino acid sequences of human, mouse, and rat were aligned and compared. The sequence data of the different subunits and species was downloaded from the public protein database UniProt Knowledgebase[1] (UniProtKB) in FASTA format. Then, the sequences for one subunit from different species were aligned using Vector NTI® software. The region against which the antibodies are directed was further analysed and the rate of identity between the species was calculated with the software.

3.2 Mutagenesis and cloning

For detection with already established antibodies as positive control, the human proteins needed to be tagged with N-terminal myc-, his- or flag-tags. Furthermore, an additional restriction site was added to be able to easily distinguish between wild type and mutant through a restriction digest. These insertions were made with the Q5® Site-Directed Mutagenesis Kit (New England Biolabs® GmbH) according to the manufactures protocol.

3.2.1 Primer design and polymerase chain reaction (PCR)

The forward and reverse primers were designed with NEBaseChanger[2]. The sequence of the target DNA fragments, the myc-, flag- oder his-tag, and the additional restriction site were added to the primer sequences. The primers are shown in Table 2.1, including the annealing temperature. To generate the needed DNA product, including the tag and additional restriction site and for amplification purposes a PCR was performed. The PCR mix was pipetted using the components supplied with the commercially available Q5® Site-Directed Mutagenesis Kit (New England Biolabs® GmbH) according to Table 3.1, the cycling conditions are shown in Table 3.2.

[1] https://www.uniprot.org/uniprot
[2] https://nebasechanger.neb.com

Table 3.1: *PCR mix*

Q5 Hot Start High-Fidelity 2x Master Mix	10µl	1x
10µM Forward Primer	1µl	0.5µM
10µM Reverse Primer	1µl	0.5µM
Template DNA (20ng/µl)	1µl	20ng
Nuclease-free water	7µl	

Table 3.2: *Cycling conditions*

Initial Denaturation	98 °C	30 sec	
Denaturation	98 °C	10 sec	25 cycles
Annealing	See Table 2.1	30 sec	
Extension	72 °C	4 min (20-30s/kb)	
Final Extension	72 °C	2 min	
Hold	4 °C	∞	

Afterwards the efficacy of the PCR reaction was controlled by gel electrophoresis using an 1% agarose gel. 2 µl of the PCR product were mixed with 2 µl of 6x Loading Dye and 8 µl water and applied onto the gel. In addition, 2 µl of the mix were set aside before PCR and served as negative control. As molecular weight marker 1 kb Plus DNA Ladder (Invitrogen™) was used. The electrophoresis was performed at 120 V for approximately 20 minutes. If the expected bands were visible at the correct height, the PCR product was transformed into *Escherichia coli* bacteria.

3.2.2 Transformation of *E. coli*

First, the samples were treated with KLD enzyme mix and incubated for 5 minutes at room temperature (RT). The used reagents were all components from the Q5® Site-Directed Mutagenesis Kit (New England Biolabs® GmbH) and the mix was pipetted according to Table 3.3.

Table 3.3: *KLD mix*

PCR Product	0.5 µl
2x KLD Reaction Buffer	2.5 µl
10x KLD Enzyme Mix	0.5 µl
Nuclease-free water	1.5 µl

Next, the transformation into competent *E. coli* XL1-blue was performed. These bacteria were already prepared and stored at -80 °C. Described in short, 100 µl of old competent *E. coli* from a previous preparation were plated onto a LB-plate containing tetracycline (see Table 2.5) and grown over night at 37°C. The next day one colony was transferred into 5 ml LB-medium with tetracycline (see Table 2.5) and incubated at 37°C and 200 rpm. After about 6 hours 200 µl of these were transferred into 10 ml LB-medium with tetracycline to get a final concentration of 1:50. The cells were incubated overnight at 37°C and 200 rpm. The next day or after not more than 16 hours 2 ml of the overnight culture was added to 100 ml LB-medium containing tetracycline and incubated at 37°C and 200 rpm until an OD_{600} of 0.5 was reached. The culture was chilled on ice for 10 minutes and afterwards centrifuged for 15 minutes at 3000 rpm and 4°C. The supernatant was discarded, and the pellets were resuspended in 10 ml ice cold TSS (see Table 2.4). 2.5 ml of sterile glycerine was added and the cells aliquoted to 200 µl per tube. The tubes were frozen with liquid nitrogen and stored at -80°C until further use.

For the transformation, 200 µl of these cells were thawed on ice for about 10 min and 5 µl of the KLD mixture or pUC18 as positive control were directly added to 100 µl XL1-blue. After an incubation time of 30 min on ice, the cells were heated to 42 °C for 50 seconds, followed by 5 min incubation on ice again. Next, 900 µl LB-medium (see Table 2.5) without antibiotic was added to each tube and the cells were incubated and shaken for 1h at 37 °C. After this step, the cells were centrifuged at 6000rpm for 5 min. 900 µl of the supernatant was discarded and the pellet was resuspended within the remaining 100 µl. All of this suspension was plated onto LB-plates containing ampicillin (see Table 2.5) and incubated overnight but not longer than 16 hours at 37 °C. For positive control about 60-600 colonies are expected.

3.2.3 DNA isolation and restriction digest

The next morning one colony was picked and transferred into 3 mL LB-medium with ampicillin and incubated again at 37 °C and 200 rpm overnight. The DNA was extracted using the QIAprep® Spin Miniprep Kit (Qiagen N.V.) according to the manufacturer's protocol. The DNA was eluted with 50 µl dH_2O and the concentration measured with a NanoDrop™ spectrophotometer (Thermo Fisher Scientific Inc.). Then, a restriction digest was performed, in order to clarify if the desired sequence (including the flanking restriction site) had been inserted into the plasmid. For this purpose, Fast Digest enzymes (Thermo Fisher Scientific Inc.) were used and mixed with the plasmids as listed in Table 3.4. The wild type plasmids served

as negative control. The digestion took 5 minutes at 37 °C followed by an inactivation of the enzymes at 80 °C, variance is possible depending on the enzymes used. 10 µl of the product was loaded onto a 1% agarose gel (see Table 2.2). The DNA fragments were separated by electrophoresis for 20 minutes at 120 V. To confirm the correct sequence of positive clones, the samples were sent to LGC genomics[3] for sequencing.

Table 3.4: *Restriction digest mix*

DNA		200 ng/µl
dH_2O	up to 17 µl	
10x Fast Digest Green Buffer	2 µl	1x
Fast Digest enzyme	0.8 µl	

3.2.4 Retransformation of *E. coli*

After ensuring that the sequences were correct, the plasmids were retransformed into competent XL1-blue as described above in chapter 3.2.2. But this time the samples were not centrifuged and just 20 µl of the suspension was plated. After incubation overnight at 37 °C one clone was picked and grown for about 6 hours in 5 ml LB-medium containing ampicillin (see Table 2.5) at 37 °C and shaken at 200 rpm. Afterwards the whole suspension was transferred to 500 ml LB-medium containing ampicillin and incubated overnight at the same conditions.

Using the QIAprep® Spin Maxiprep Kit (Qiagen N.V.), the DNA was extracted the next day according to the manufacturer's protocol. The DNA was resuspended in TE-Puffer (see Table 2.3) and diluted to a final concentration of 1.0 µg/µl.

3.2.5 Protocol for CHRFAM7A-flag

Since the generation of CHRFAM7A-flag using the Q5® Site-Directed Mutagenesis Kit (New England Biolabs® GmbH) (as describe in chapter 3.2.1) was not successful, a new cloning method was chosen. This time the flag-tag-sequence was included into the forward primer. The PCR mix was pipetted as described above (see Table 3.1) and the cycling conditions were the same as in Table 3.2, but this time 35 cycles of denaturation, annealing and extension were

[3] https://www.lgcgroup.com

performed instead of 25. In order to remove the template added during the PCR reaction, all of the PCR-product was mixed with 2 µl 6x loading dye and loaded onto the 1% agarose gel. Conditions for gel electrophoresis were the same as described above. The bands were excised with a scalpel and the DNA was recovered with the Zymoclean™ Gel DNA Recovery Kit (Zymo Research Corp.) according to the manufacturer's protocol. Afterwards the PCR product was digested and ligated into the pUNIV expression vector. For that purpose, two different restriction digests were prepared according to Table 3.5 and Table 3.6. These mixtures were incubated for 10 minutes at 37 °C, followed by an inactivation for 5 minutes at 80 °C. To dephosphorylate the vector, its digestion product was mixed with an alkaline phosphatase according to Table 3.7 and incubated for 30 minutes at 37 °C.

Next, all products were applied onto a 1% agarose gel, separated by electrophoresis for 25 minutes at 100 V. The bands were excised and purified with the GFX™ PCR DNA and Gel Band Purification Kit (GE Healthcare GmbH) according to the manufacture's protocol. After that, the ligation was performed. The products were mixed with the ligase as listed in Table 3.8 and incubated for 1 hour at RT, followed by an inactivation at 65 °C for 10 minutes. Afterwards the transformation, isolation, restriction digest and retransformation were performed as described above.

Table 3.5: *Digestion mix with insert*

Insert (purified PCR-Product)	10 µl
10x Fast Digest Green Buffer	1 µl
MluI	0.8 µl
XhoI	0.8 µl

Table 3.6: *Digestion mix with vector*

dH_2O	31 µl
Vector (pUNIV, c= 1µg/µl)	3 µg
10x Fast Digest Green Buffer	1 µl
MluI	0.8 µl
XhoI	0.8 µl

Table 3.7: *Dephosphorylation mix*

Digested vector	~40 µl
Alkaline Phosphatase 10x Reaction buffer (Promega GmbH)	5 µl
Calf-intestinal alkaline phosphatase (CIAP/CIP) (Promega GmbH)	2 µl

Table 3.8: *Ligation mix*

dH_2O	2 µl
Insert or dH_2O as negative control	2 µl
Vector	4 µl
T4 Buffer	1 µl
T4 Ligase	0.8 µl

3.3 HEK cells cultivation and transfection

HEK-293 cells were transfected with the cloned plasmids and used in western blot and immunocytochemistry experiments. The cells were kept in 10 cm dishes in "HEK complete medium" (see Table 2.6) and split twice a week. For a 4-day period 0.5 million cells were seeded in 10 ml medium and for a 3-day period 1 million cells. The cells were incubated at 37 °C and 5 % CO_2.

For western blot experiments, 1 million cells were seeded in 9 ml medium on Day 0, transfected via calcium phosphate precipitation on Day 1 and harvested on Day 3. For the transfection 21 µg DNA were mixed with 50 µl $CaCl_2$ and 429 µl water and dropped into HeBS buffer (see Table 2.7) under air bubbling. The DNA of the different subunits was already mixed before in a ratio of 1:1. The mix was vortexed and after 20 minutes incubation time, the mix was vortexed again and 1 ml was dropped onto each 10 cm dish. After a maximum of 5 hours the cells were washed twice with PBS (see Table 2.8) and 10 ml fresh medium was added. Before harvesting, the cells were washed with 5 ml PBS and then with 1 ml PBS, scraped off the dishes and collected in reaction tubes. Afterwards the cell suspension was centrifuged at 13000 rpm at 4 °C for 20 min and a membrane preparation (see chapter 3.4) was performed.

For immunocytochemistry, 0.1 million cells were seeded in 500 µl medium on PDL coated 1.3 cm coverslips, prepared in a 24 well plate on Day 0. On Day 1 the cells were transfected with

500 ng DNA and Metafectene® Pro (Biontex Laboratories GmbH), diluted in PBS. The DNA of the different subunits and the chaperons was mixed before in a ratio of 1:1. The next day the cells were fixed and further treated as described in chapter 3.6.

3.4 Membrane preparation

Transfected HEK cells as well as mouse and rat brain tissue were prepared for further use through membrane preparation. For that, 500 µl of homogenisation buffer (see Table 2.9) were added to the cells/tissue and the sample was treated with an ultrasonic pulse at a power level of 10% for 5 seconds. If there were pieces left, another pulse was given. After centrifugation at 13000 rpm at 4 °C for 30 min, the supernatant was discarded and the steps were repeated with washing buffer (see Table 2.10), but a 30 min incubation time before centrifugation was added. Afterwards, the pellet was homogenised again in washing buffer and divided into an appropriate number of tubes for further use. Usually, HEK cells were divided into 0.5 plates per tube and tissue to about 100 µg per tube. All reagents and samples were kept on ice during the steps. The samples were stored at -20 °C until further use. Protein concentration was measured with Pierce™ BCA Protein Assay Kit (Thermo Fisher Scientific Inc.) and the GloMax® Plate Reader (Promega GmbH).

3.5 Western blot

Western blot technique was used to test the specificity and ability of the antibodies to detect the subunits in rat and mouse brain tissue as well as in transfected HEK cells. For that, 10% Tris – Glycine separating gels and 5% stacking gels were mixed according to Table 2.11 and poured into gel cassettes.

The separating gel hardened for one hour and the stacking gel for 30 minutes. The pockets were washed twice with running buffer (see Table 2.15) and filled with it.

When tissue or HEK cells were used as samples, the pellets from membrane preparation were resuspended in 1x sampling buffer (see Table 2.20) through ultrasonic pulse at a power level of 10% for a maximum of 5 seconds. All other samples and markers were just diluted in sample buffer to a desired concentration. After that, the proteins were denatured by heating to 65 °C for 15 minutes and centrifuged up to 60 seconds at 5000 rpm, except the marker (see Table 2.23).

20 µl of the samples were loaded onto the gel, when a 12-well comb was used. When the 15-well comb was used, only 10 µl were loaded. With electrophoresis at 200 V and 200 mA for

about 50 minutes the proteins were separated. Afterwards, the transfer to a methanol activated PVDF membrane was performed using the Trans-Blot® Turbo™ Transfer System from Bio-Rad Laboratories and transfer buffer (see Table 2.16) to keep the membrane and gel wet. To block unspecific protein binding the membrane was incubated for 30 minutes in 5% blocking buffer (see Table 2.18) before incubating overnight with the primary antibody (dilution see Table 2.21). The next day, the membranes were washed 4 times with 1.5% washing buffer (see Table 2.19) and incubated for 1 hour with the secondary antibody (dilution see Table 2.22). After another washing step, the membrane was incubated for 5 minutes with 4 ml of Millipore Immobilon Western Chemiluminescence HRP Substrate. Visualisation and pictures were made with the Bio-Rad ChemiDoc™ Imager.

3.6 Immunocytochemistry (ICC)

The antibodies were also characterised and tested in immunocytochemistry. As described in chapter 3.3, HEK cells were transfected with the plasmids containing the DNA of the subunits of interest. The day after the transfection the cells were fixed with 4% paraformaldehyde for 15 minutes at RT and washed three times with 1x PBS (see Table 2.17). Unspecific binding was blocked through incubation with blocking solution (see Table 2.24) for 1 hour. After another washing step the cells were incubated overnight at 4 °C with the primary antibody (see Table 2.26) diluted in dilution solution (see Table 2.25) or PBS (see Table 2.17) if the antibody should be stored again afterwards and reused.

The next day the primary antibody was removed, and the cells washed again with PBS (see Table 2.17) before the secondary antibody (see Table 2.27) was added. Different secondary antibodies with different wavelengths were chosen depending on the primary antibody. These antibodies were diluted 1:1000 in PBS (see Table 2.17) and incubated for an hour in the dark. Next, the cells were washed with 0,02% Tween 20 PBS (see Table 2.17) and mounted with Prolong™ Glass Antifade Mountant with NucBlue™ Stain (Thermo Fisher Scientific Inc.) on glass slides. The slides were imaged using a confocal microscope from Carl Zeiss AG (880LSM). Wavelengths of the lasers used for excitation were 405nm, 488nm and 561 nm.

To check if the transfection worked, GFP and DsRed were used as positive control. The transfection was performed as described above using the plasmids pEGFP-C1 and pDsRed-C1 (both from Clontech Laboratories Inc.). The proteins encoded by this plasmid, GFP and DsRed, exhibit flourescence in the green and red channel when excited and do not need to be treated

with antibodies to be detected. Therefore, it is just a positive control for transfection and imaging but not for the staining.

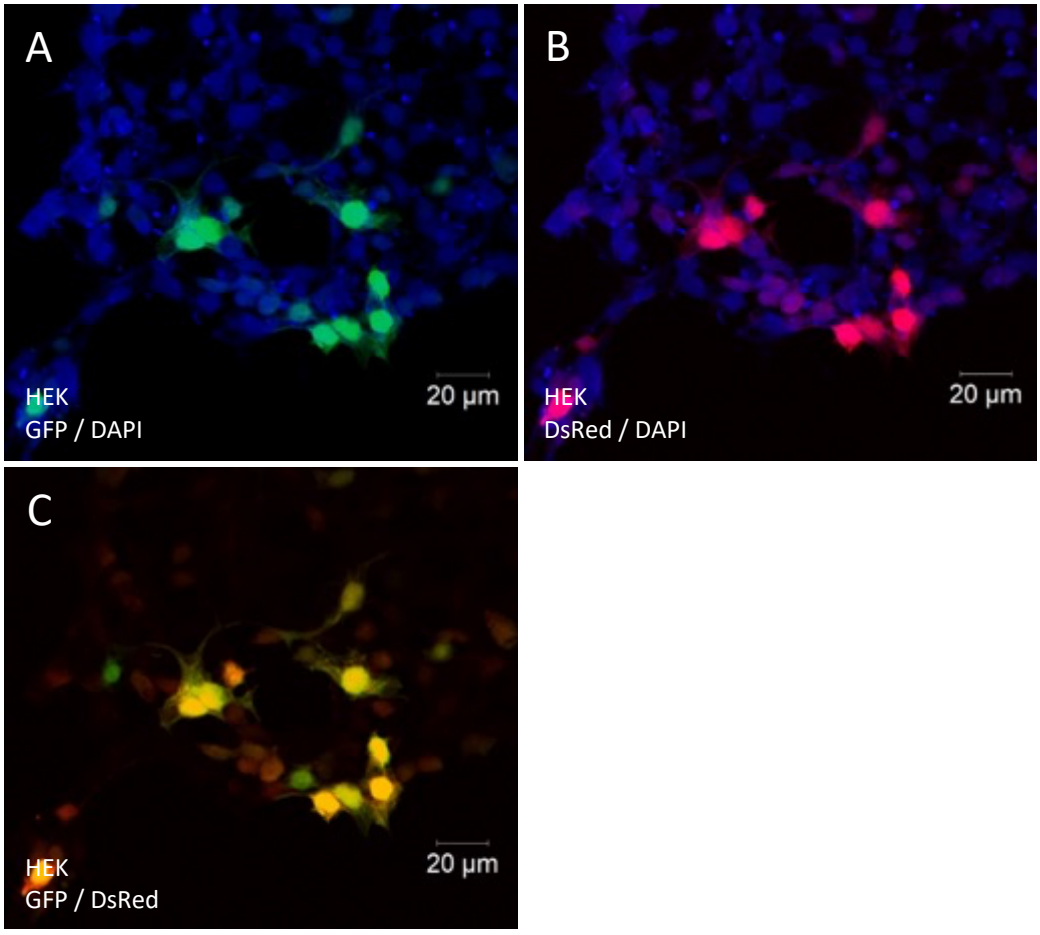

Figure 3.1: *HEK cells transfected with GFP and DsRed, stained with DAPI as positive control for ICC. DAPI staining and GFP (panel A), DAPI staining and DsRed (panel B), overlay of GFP and DsRed (panel C).*

4 Results

The results of this work are structured in two main parts according to the two different aims of this study (see chapter 1.6).

On the one hand, there are the already established antibodies against the α3, α4, β2 and β4 subunit [47]. On the other hand, antibodies against the α7 subunit and its duplications needed to be newly generated. For a better understanding an overview of these antibodies is given below.

4.1 New generation of anti-α7 antibodies

As already mentioned in chapter 1.5, our group previously generated a new generation of eight different anti-α7 antibodies. These antibodies are directed against different parts of the amino acid sequence of the subunits, as pictured in Figure 4.1. The first ones, termed α7N S1 and S2 are directed against a sequence of about 30 aa at the N-terminus of the full-length α7, a sequence the duplicated subunits are missing. Therefore, those antibodies should only recognize the full-length protein. Next, the so termed α7L S3 and S4 antibodies should recognize all of the three proteins, as they were generated against a sequence from the loop region, which is the same in all of the α7-subunits. To detect the duplicates, four antibodies were generated, dupα7N S5 and S6 on the one hand and 2bpα7N S7 and S8 on the other. These are directed against the N-terminus of dupα7 and dup$\Delta\alpha$7 respectively. Specificity between these antibodies should be given because of the differences in translation, which were already explained in chapter 1.3.2.

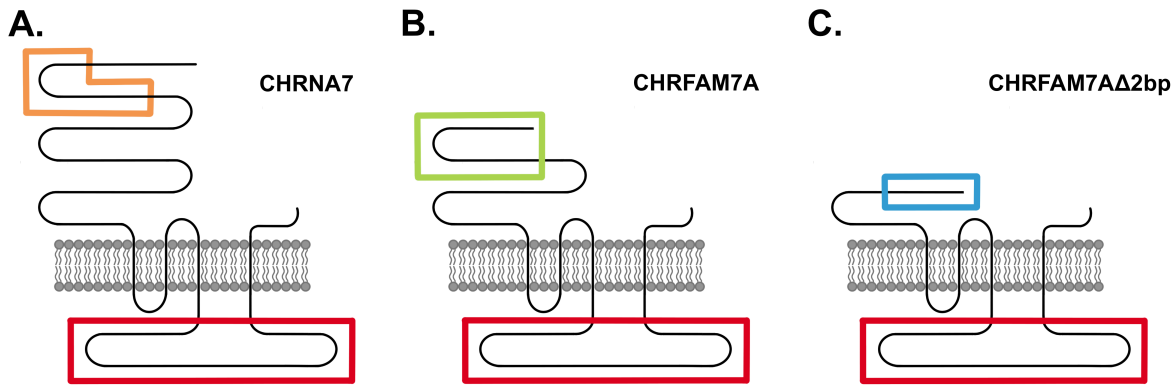

***Figure 4.1**: Targets of the newly generated anti-α7 antibodies.*
A. Full-length α7 subunit. The target of α7N S1 and S2 is shown in orange and the target of α7L S3 and S4 is shown in red. B. Gene product of CHRFAM7A. The target of dupα7N S5 and S6 is shown in green and the target of α7L S3 and S4 is shown in red. C. Gene product of CHRFAM7AΔ2bp. The target of 2bpα7N S7 and S8 is shown in blue and the target of α7L S3 and S4 is shown in red.

The immunised rabbits received four booster immunisations and after the third one, the first blood samples were already taken. The blood was taken weekly and purified with affinity chromatography columns. Afterwards the samples were pooled and tested. The antibodies were named after the rabbit with S1-S8 and additionally numbered with the blood draw §3/1 to §3/3. This work is focused on the results of the antibodies gained after the third immunisation, since the final immunisation and purification of further blood samples followed after this work was finished.

4.2 Prediction of antibody binding by amino acid alignments

4.2.1 Subunits of α3β4 and α4β2 receptors

The first aim of this study was to investigate, whether antibodies directed against the mouse α3, α4, β2 and β4 subunits recognise the human proteins as well. Therefore, the amino acid sequences of the fragments used for immunisation were compared between rat and human by amino acid alignments to get an impression of their similarity. The results were needed to make a prediction on how likely it is that the antibodies would recognise the proteins of the other species. In Figure 4.2 – 4.5, the results of the amino acid alignments and rate of identity of the sequences are shown. Here, it must be mentioned, that the given positions are from the mouse sequences and could be shifted in the alignment because of added amino acids at the beginning of the human sequences.

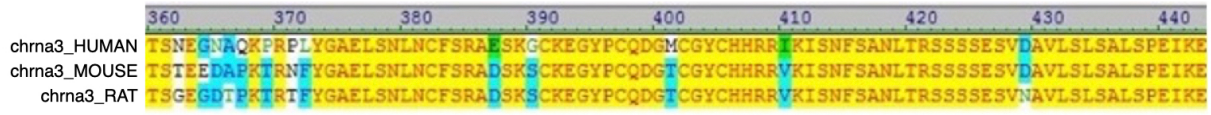

Figure 4.2: *Alignment of mouse, rat and human amino acid sequences of the α3 subunit used for immunisation. Differences are marked in white, green and blue; matches are marked in yellow. Position: amino acids 354-437 (TSTE…EIKE), identity: 84.5%*

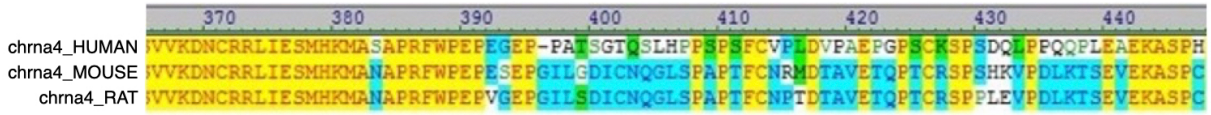

Figure 4.3: *Alignment of mouse, rat and human amino acid sequences of the α4 subunit used for immunisation. Differences are marked in white, green and blue; matches are marked in yellow. Position: amino acids 365-446 (VVKD…ASPC), identity: 53.7%*

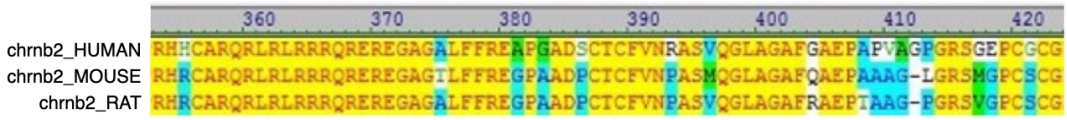

Figure 4.4: *Alignment of mouse, rat and human amino acid sequences of the β2 subunit used for immunisation. Differences are marked in white, green and blue; matches are marked in yellow. Position: amino acids 353-422 (RHRC…CSCG), identity: 76.1%*

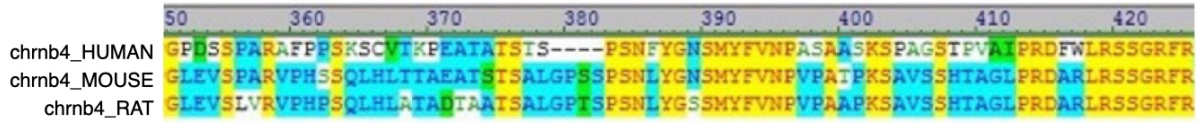

Figure 4.5: *Alignment of mouse, rat and human amino acid sequences of the β4 subunit used for immunisation. Differences are marked in white, green and blue; matches are marked in yellow. Position: amino acids 350-424 (GLEV…GRFR), identity: 44.0%*

Based on these alignments it was expected that antibodies against the mouse sequence of the α4 and β4 subunit may not recognise the human subunits, as the identity of the sequences is only 53.7% for α4 and 44.0% for β4. In contrast to that, the α3 and β2 subunits have a much higher rate of identical amino acids with 84.5% for the α3 subunit and 76.1% for the β2 subunit. Therefore, positive results would be expected.

4.2.2 The α7 subunit

Antibodies against the α7 subunit are gained from rabbits immunised with proteins containing amino acid sequences from the human subunits, as described in chapter 4.1. Therefore, the alignments were needed to examine, if the antibodies could also recognise the proteins in tissue from mice and rats used in western blot. The results are shown in Figure 4.6 and Figure 4.7. The N-terminus of the α7 nAChR subunit is 100% similar in all three species. The loop region has some differences between amino acid 370 and 379 and amino acid 393 and 398, but with an identity of 83.5% positive results could be expected.

Figure 4.6: *Alignment of mouse, rat and human amino acid sequences of the N-terminus of the α7 subunit, which is the sequence used for antibody generation in the rabbits S1 and S2.*
Differences are marked in white, green and blue; matches are marked in yellow. Position: amino acids 30-56 (YKEL…VYFS), identity: 100%

Figure 4.7: *Alignment of mouse, rat and human amino acid sequences of the loop region of the α7 subunit, which is the sequence used for antibody generation in the rabbits S3 and S4.*
Differences are marked in white, green and blue; matches are marked in yellow. Position: amino acids 349-433 (GEDK…DPDL), identity: 83.5%

As the duplicated subunits dupα7 and dup$\Delta\alpha$7 are only found in humans, the antibodies against these subunits were only tested with HEK cells transfected with the human DNA sequences and alignments were not needed and could not be done.

4.3 Mutagenesis and cloning

As described in chapter 3.2 all constructs were created using the Q5® Site-Directed Mutagenesis Kit (Thermo Fisher Scientific Inc.), except β4-flag, dupα7-flag and dup$\Delta\alpha$7-his. The chosen method did not work for these three constructs. After the PCR-reaction, no product was visible on the control gel and only wild type colonies of *E. coli* grew on the culture plate. Therefore, new primers were designed (listed in Table 2.1) and the methods were improved. For the dup$\Delta\alpha$7 construct, the new primers and an adjustment of the incubation time for the KLD mix to one hour instead of 5 minutes already yielded successful results.
However, the mutation within the sequence of dupα7 was still not successful, although the adjustment was done. Therefore, a new protocol needed to be designed as described in chapter 3.2.5. This time the sequence for the flag-tag was included into the forward primer, and the PCR product, which newly contained the tag-sequence at the 5’ end was ligated into an expression vector. For the β4 subunit, however, the right conditions to add the tag have not been found yet.

4.4 Western blot

The next step was the confirmation of the sequence alignments (as described in chapter 3.1) using selected experimental methods. First, the antibodies were tested in western blot. Therefore, a design of blots, that could be applied for every antibody and allows a comparison to each other, was established. On the one hand, brain tissue from wild type and the corresponding knockout mice was used to test the specificity of the antibodies. Since α3 and β4 are only expressed in selected regions of the CNS, tissue from habenula was chosen in which all four subunits of interest are expressed in significant amounts. As there were no α3

and α4 knockout mice available, β2- and β4-knockout tissue were used instead to test the antibodies against these subunits, based on the outcome of a study, which showed that assembling subunits are similarly decreased in knockout mice (see chapter 5) [53]. Additionally, the antibodies were tested on habenula brain tissue from wild type rats.

On the other hand, transfected HEK cells were used in experiments investigating the comparison of rodent and human α3, α4, β2 and β4 subunits. The cells were transfected with plasmids containing the mouse sequences as well as plasmids containing the human sequences, to compare them to each other. In addition, transfected HEK cells were needed to characterise the newly generated antibodies against the α7 subunit and its duplicates, as these were directed against the human sequences. Untransfected HEK cells were used as a negative control.

4.4.1 α3S1, β2S19 and β4S5 antibodies

The most promising already established antibodies were α3S1, β2S19 and β4S5 [47]. Therefore, these antibodies were tested in detail using the concentration and sample schema carried out before. To optimise the western blots for these antibodies, different concentrations of HEK cells and brain tissue were tested.

First, a blot with rat and mouse habenula was designed, using a protein concentration between 20 to 40 µg per lane. The results (Figure 4.8) show that 20 µg of mouse habenula tissue are enough for detection with β2S19, but 30 µg should be used for β4S5. The concentration of rat tissue needs to be higher for both antibodies. For detection with β2S19 40 µg should be enough, but for β4S5 more than 40 µg have to be applied and tested again.

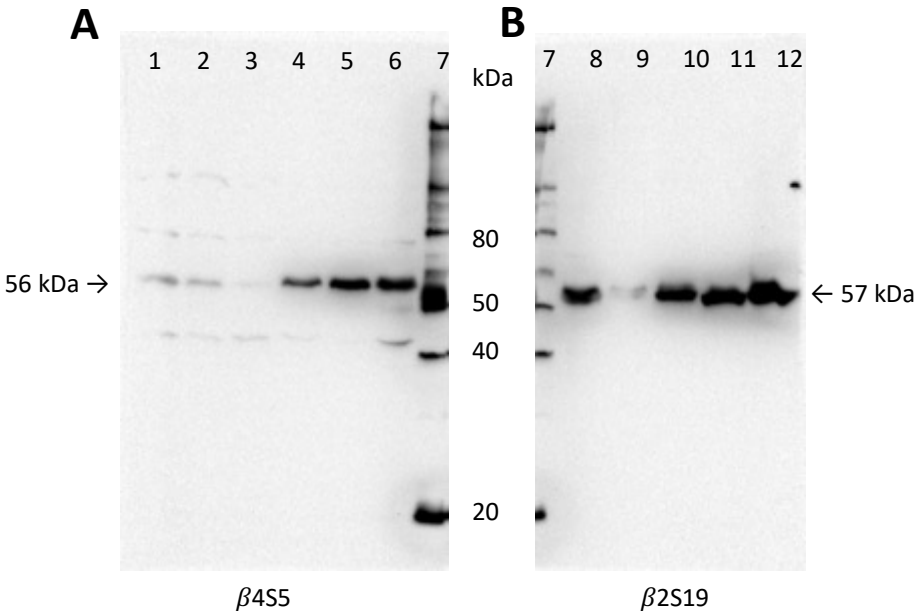

Figure 4.8: *Western blot with different concentrations of mouse and rat brain tissue, incubated with β4S5 antibody (A) and β2S19 antibody (B).*
Lane 7: protein standards Magic Mark™ 1:35 and Blue Plus® 1:6. Lanes 1-3: rat habenula with a protein concentration of 40 µg (lane 1), 30 µg (lane 2) and 20µg (lane 3). Lanes 4-6: wt mouse habenula with a protein contentration of 20 µg (lane 4), 30 µg (lane 5) and 40 µg (lane 6). Lanes 8-9: rat habenula with a protein concentration of 40 µg (lane 8) and 20µg (lane 9). Lanes 10-12: wt mouse habenula with a protein contentration of 20 µg (lane 10), 30 µg (lane 11) and 40 µg (lane 12). Detected with an exposure time of 120 seconds.

For HEK cells, different dilutions were prepared and applied to the gel to find the optimal concentration for a clear band at an exposure time of 60 to 120 sec. The previous prepared and pelleted cells were diluted in sample buffer and therefore the given concentrations were measured in fractions of a 10 cm culture dish of HEK cells. Starting with 1:20 of a culture dish, the final concentration was found between 1:80 and 1:500 of a culture dish, depending on the DNA transfected and the antibody used for detection.

In Figure 4.9 the results regarding the question whether the antibodies recognise the human and mouse proteins equally, are shown. The expected bands are visible at about 58 kDa for the α3 subunit, at 57 kDa for β2 and at 56 kDa for β4. The β4S5 antibody gave no band for HEK cells transfected with human α3β4 and therefore does not bind the human protein. But the other two antibodies show equal bands at the same height for mouse and human α3β4 or α4β2, which confirmed the results from the amino acid alignment.

In brain tissue from wild type mice and rats the specific subunit was recognised by all antibodies, but in a different intensity. The β2S19 antibody recognises the lowest concentration of protein, β4S5 needs the highest, especially for tissue from rats. The samples from knockout mice gave no band in all blots, as expected. This means that all antibodies are

specific for their subunit in brain tissue and also suitable for both, human and mouse proteins, except for β4S5 which can't be used to detect human proteins.

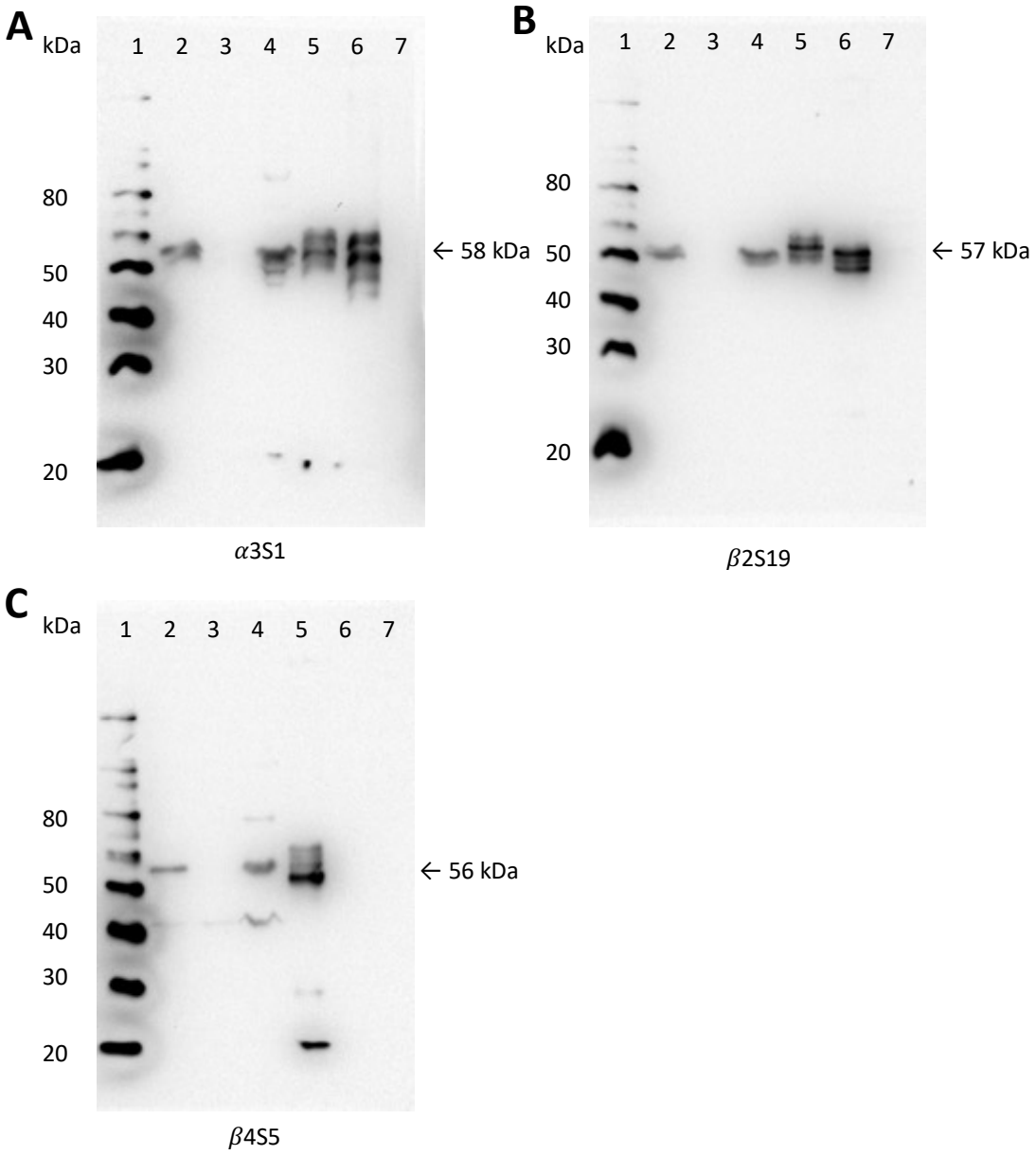

Figure 4.9: *Western blots incubated with α3S1 (A), β2S19 (B) and β4S5 (C) antibodies.*
Lane 1: molecular weight marker Magic Mark™ in a dilution of 1:40. Lane 2: 30 µg (A+C) or 20 µg (B) of habenula from wt mice. Lane 3: 20 µg of habenula from ko mice (β4-ko for α3S1 and β4S5 (A+C) and β2-ko for β2S19 (B)). Lane 4: 94 µg (A+C) or 40 µg (B) of rat habenula. Lane 5: HEK cells in a dilution of 1:500 transfected with mα3β4 (A+C) and mα4β2 (B). Lane 6: HEK cells transfected with hα3β4 (A+C) in a dilution of 1:80 and hα4β2 (B) in a dilution of 1:200. Lane 7: untransfected HEK cells diluted 1:80 in A and C, diluted 1:200 in B. Detected with an exposure time of 60 seconds.

4.4.2 α4S26 antibody

Keeping the alignments in head, expectations for the anti-α4 antibody to be able to detect the human subunit were low. In Figure 4.10 the result of the western blot incubated with the

α4S26 antibody is shown. There are no bands visible at the lanes containing brain tissue, except an unspecific band at the lane with tissue of knockout mice, which speaks against the specificity of this antibody. Although the antibody did detect the α4 subunit from mouse in transfected HEK cells at the expected size of 70kDa. Nevertheless, it did not recognise the human protein. Also, the exposure time of the blot shown was very short, but even a picture made after 180 seconds did not show more bands.

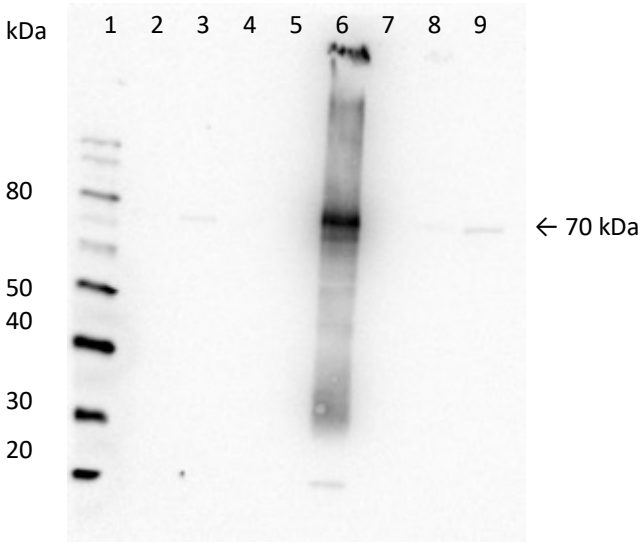

Figure 4.10: *Western blot incubated with α4S26 antibody.*
Lane 1: molecular weight marker Magic Mark™, diluted 1:25. Lanes 2-4: 20 µg of habenula from wt mice (lane 2), β2-ko mice (lane 3) and rats (lane 4) per lane. Lanes 6, 8: HEK cells transfected with mα4β2 (lane 6) and hα4β2 (lane 8) in a dilution of 1:20. Lane 9: untransfected HEK cells in a dilution of 1:5. Lanes 5 and 7 do not contain any samples and were filled with sample buffer. Detected with an exposure time of 10 seconds.

4.4.3 β4S4, β4S6 and β4S22 antibodies

For the β4 subunit four different antibodies were tested and compared. The first one, β4S5, gave the best results, which are already described in chapter 4.4.1. The results for the other ones are shown in Figure 4.11. β4S4 did not only stain the expected bands in wild type and rat brain tissue, but also gave unspecific bands in tissue from knockout mice at lower molecular weight as well. Bands for the human β4 subunit are not visible at any blot, which is not surprising considering the alignments. HEK cells transfected with the DNA of the subunits from mouse gave intense bands in every blot.

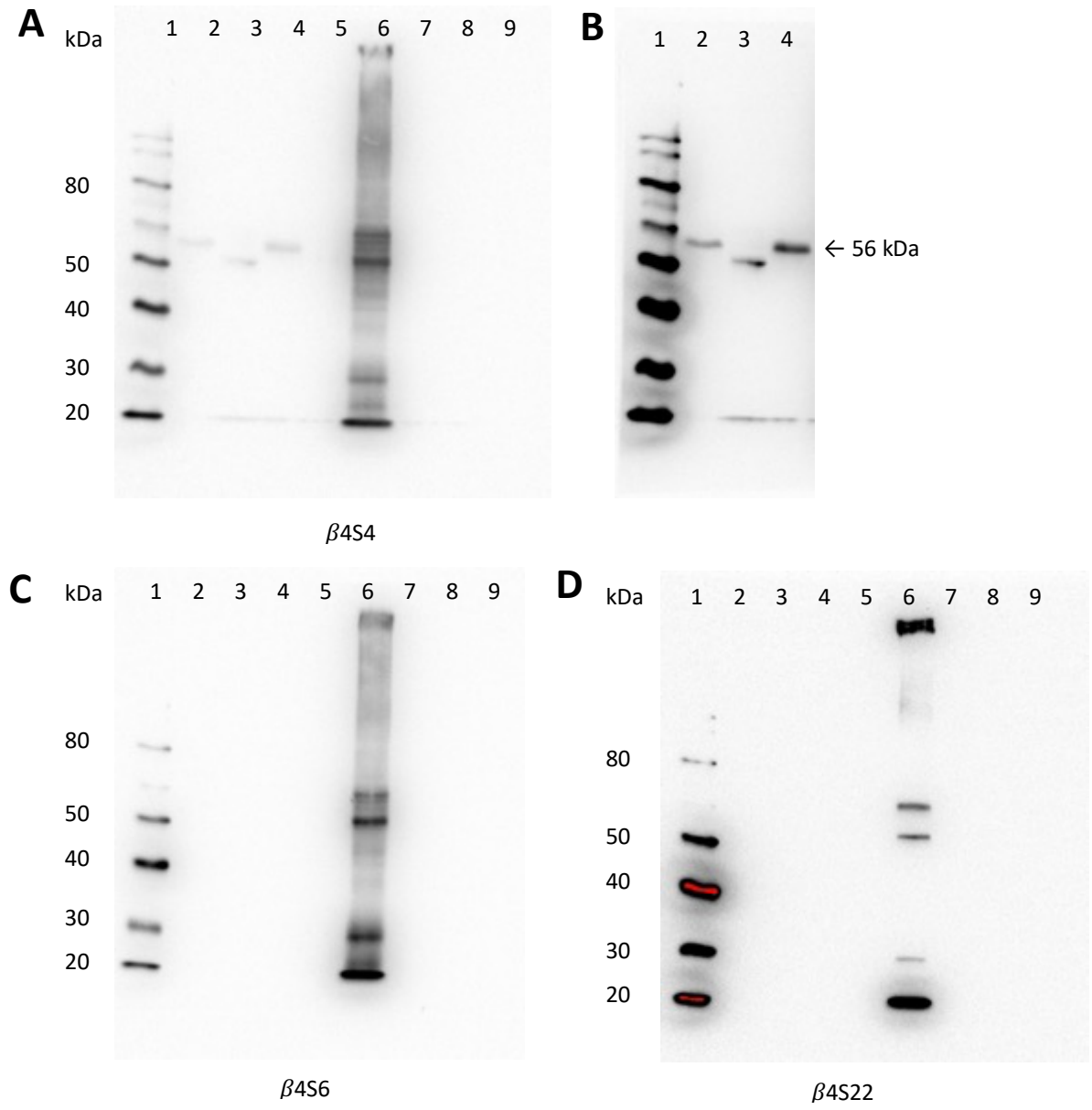

Figure 4.11: *Western blots incubated with different β4 antibodies: β4S4 (A+B), β4S6 (C) and β4S22 (D). Panel B shows the first four lanes from the same blot shown in panel A, but with a higher exposure time. The exposure time for detection is either 5 seconds (A) or 30 seconds (B-D).*
The samples are always put onto the gel in the following schema. Lane 1: molecular weight marker Magic Mark™ (1:25). Lane 2-4: 20 µg of habenula from wt mice (lane 2), from β4-ko mice (lane 3) and from rats (lane 4) per lane. Lane 6: HEK cells transfected with mα3β4 (1:20). Lane 8: HEK cells transfected with hα3β4 (1:20). Lane 9: untransfected HEK cells (1:5). Lanes 5 and 7 do not contain any samples and were filled with sample buffer.

4.4.4 New generation of anti- α7 antibodies

To characterise the new generation of anti-α7 antibodies with western blot, HEK cells were transfected with different combinations of plasmids containing the DNA of the α7 and the duplicated subunits. On the one hand, there are the different subunits alone, α7, dupα7 and dup$\Delta\alpha$7, and on the other hand, there are combinations of dupα7 or dup$\Delta\alpha$7 with the full-

length α7, since there is the hypothesis that the duplicated subunits won't form a receptor on their own and need to co-assemble with α7 (see chapter 1.3.2). Additionally, plasmids containing the DNA sequences of the chaperons NACHO and RIC-3 were added to all combinations. All of the blots followed the same scheme including all of the combinations, regardless which antibody was used. As positive control, a blot was incubated with a mixture of anti-myc, -flag and -his antibodies, as the plasmids were all tagged with one of these protein-tags. HEK cells transfected with $\alpha 3\beta 4$ from mice were used as additional positive control for the anti-myc and -flag antibody. As negative control, untransfected HEK cells were applied to the last lane.

In Figure 4.12 the western blot incubated with the α3L S3 antibody is shown. Unfortunately, there are no bands visible at the lanes containing rat and mouse hippocampus brain tissue. The hippocampus contains the highest density of a-Bungarotoxin binding sites [24] and is therefore expected to be especially rich in a7-nAChRs. The lanes containing HEK cells transfected with the different α7 combinations are heavily overloaded, but the most intense bands are at the expected height for the protein size, which is 56 kDa for the full-length α7, 45 kDa for dupα7 and 39 kDa for dup$\Delta\alpha$7. Additionally, there are no bands in lane 10 and 11 visible, as expected.

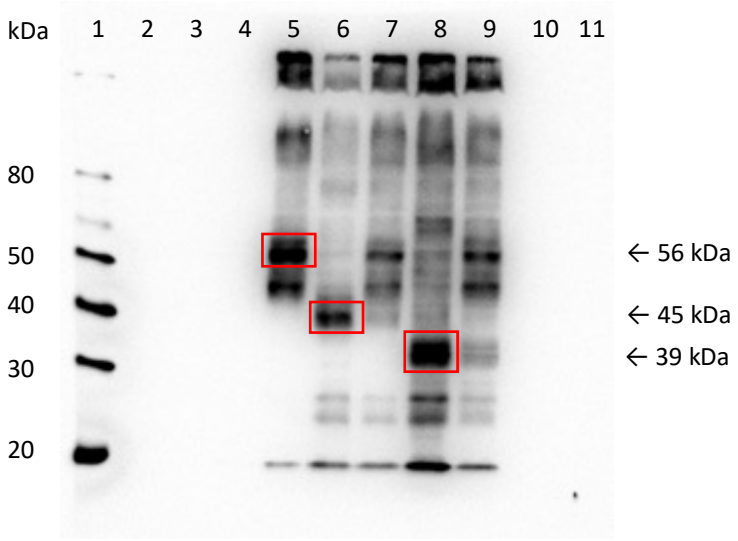

Figure 4.12: *Western blot incubated with α7L S3 antibody.*
Lane 1: molecular weight marker Magic Mark™ in a dilution of 1:40. Lanes 2-4: 20 µg of hippocampus from wt mice (lane 2), hippocampus from α7 ko mice (lane 3) and hippocampus from rats (lane 4) per lane. Lane 5-9: HEK cells transfected with different combinations of α7 subunits and the chaperons Nacho and RIC-3 in a dilution of 1:20. Lane 5: HEK cells transfected with CHRNA7. Lane 6: HEK cells transfected with CHRFAM7A. Lane 7: HEK cells transfected with CHRNA7 and CHRFAM7A. Lane 8: HEK cells transfected with CHRFAM7AΔ2bp. Lane 9: HEK cells transfected with CHRNA7 and CHRFAM7AΔ2bp. Lane 10: HEK cells transfected with m$\alpha 3\beta 4$ in a dilution of 1:20. Lane 11: untransfected HEK cells in a dilution of 1:20. Detected with an exposure time of 10 seconds.

All of the other tested antibodies gave no or just unspecific bands and are therefore not shown.

4.5 Immunocytochemistry

The second method chosen for characterisation of the antibodies was immunocytochemistry. HEK cells were transfected and stained as described in chapter 3.6. As positive control the cells were additionally stained with anti-myc, anti-flag and anti-his antibodies, depending on the tag that was inserted in the particular subunit. These antibodies were detected with a secondary anti-mouse antibody, which is conjugated to Alexa Flour® 568 and therefore shown in red in the following pictures. The α3S1 and β2S19 antibody as well as the new anti-α7 antibodies were detected with a secondary anti-rabbit antibody, which is conjugated to Alexa flour® 488 and therefore shown in green. Cells only stained with DAPI (in blue) are not transfected and serve as negative control.

4.5.1 α3S1 antibody

HEK cells transfected with the DNA of β4 and myc-tagged α3 subunits from mice on the one hand and from human on the other, were stained with the α3S1 antibody and compered to each other. The results of the immunocytochemical staining are shown in Figure 4.13. Nearly all cells stained with the anti-myc antibody (panels B and E) are also stained with α3S1 (panels A and D) in both conditions. This would mean that the α3S1 antibody is specific for the α3 subunit, since the positive control is meant to stain all cells that have expressed receptors containing myc-tagged α3.

Further, there is no difference in staining intensity between the cells transfected with murine or human subunits. Also, the number of cells stained was approximately the same. Therefore, it can be assumed that the antibody recognises the proteins equally well. The transfection rate seems to be similar in both conditions.

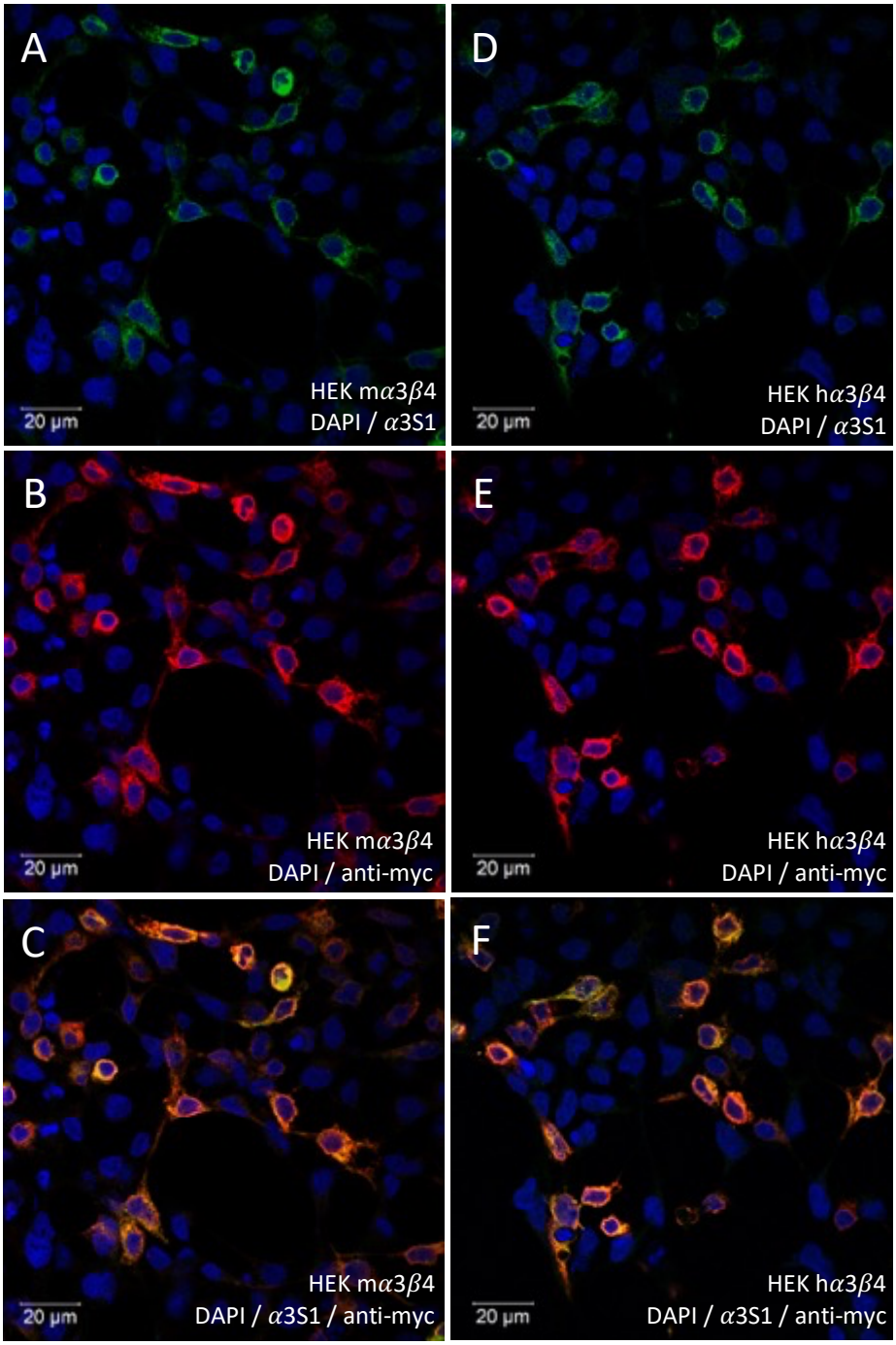

Figure 4.13: *HEK-293 cells transfected with a plasmid containing the myc-tagged CHRNA3 and flag-tagged CHRNB4 and stained with the antibody α3S1.*
Panels A-C: Cells transfected with the DNA of mouse subunits and stained with DAPI, the α3S1 antibody (panel A) and anti-myc 4A6 as positive control (panel B), overlay (panel C). Panels D-F: Cells transfected with the DNA of human subunits and stained with DAPI, the α3S1 antibody (panel D) and anti-myc 4A6 as positive control (panel E), overlay (panel F).

4.5.2 β2S19 antibody

The results for β2S19 are very similar to the ones for the α3S1 antibody. This time, HEK cells were transfected with the DNA of the murine or human myc-tagged α4 and flag-tagged β2 subunit and stained with β2S19 and an anti-flag antibody as positive control. Nearly all cells

stained with the anti-flag antibody (Figure 4.14, panels B and E) are also stained with β2S19 (Figure 4.14, panels A and D), which indicates the specificity of the antibody for this subunit. Since there is almost no difference in staining intensity and the number of stained cells, it can be assumed that β2S19 is recognising the subunit from mice as well as the human subunit. Also, the transfection rate seems to be similar in both conditions.

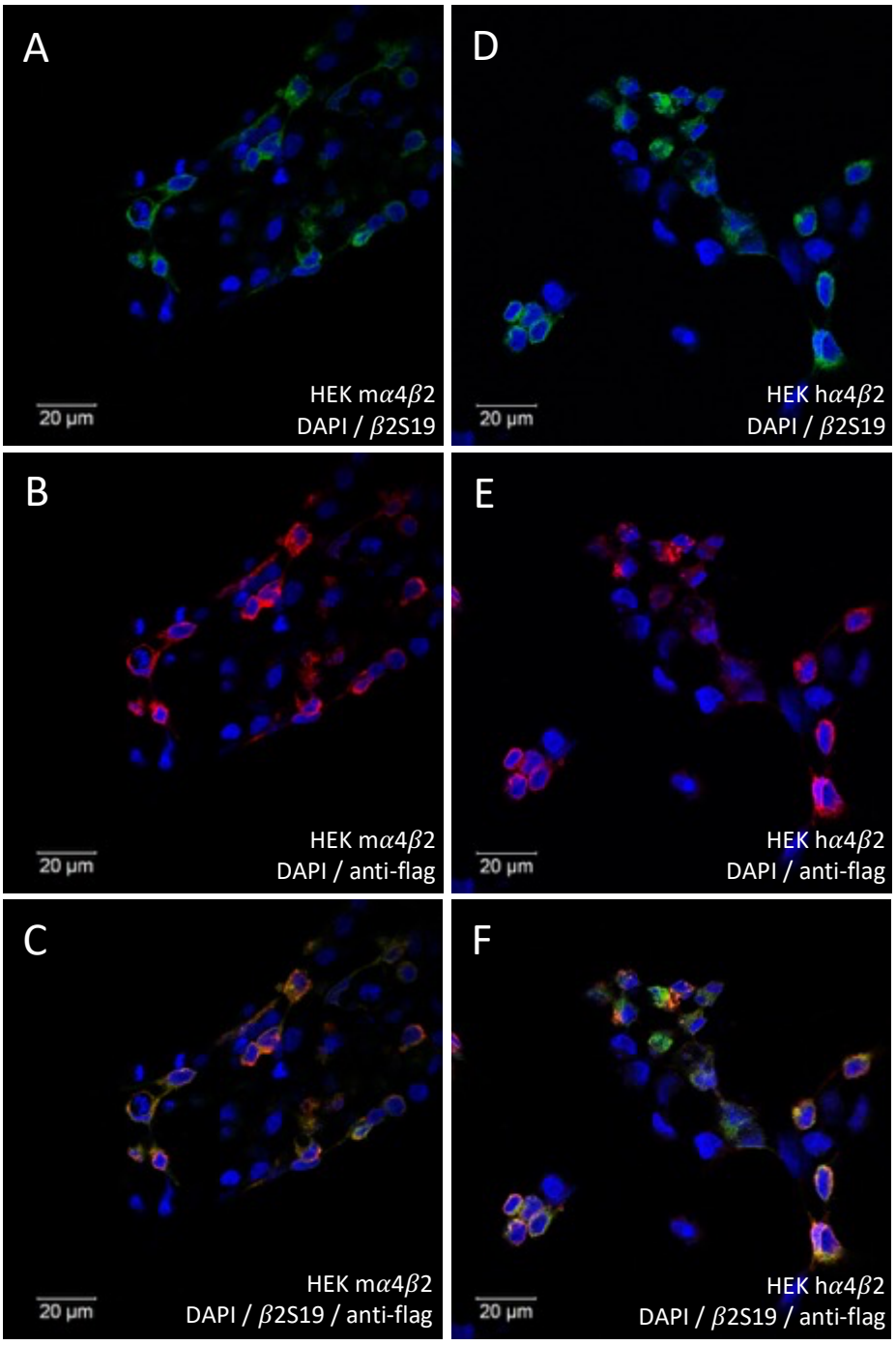

Figure 4.14: *HEK-293 cells transfected with a plasmid containing the myc-tagged CHRNA4 and flag-tagged CHRNB2 and stained with the antibody β2S19.*
Panels A-C: Cells transfected with the DNA of mouse subunits and stained with DAPI, the β2S19 antibody (panel A) and anti-flag F9291 as positive control (panel B), overlay (panel C). Panels D-F: Cells transfected with the DNA of human subunits and stained with DAPI, the $\alpha\beta$2S19 antibody (panel D) and anti-flag F9291 as positive control (panel E), overlay (panel F).

4.5.3 New generation of anti- α7 antibodies

In the following the results for α7N S1, α7L S3 and S4, dupα7N S5 and 2bpα7N S7 in immunocytochemistry are shown and described in detail. All other antibodies were not tested in ICC yet.

As positive control different antibodies for the different constructs were chosen. The α7 subunit contains a myc-tag, the dupα7 construct is flag-tagged and the dup$\Delta\alpha$7 construct has a his-tag. Therefore, the anti-myc antibody 4A6 was used to detect the α7 subunit. For the dupα7 construct, the anti-flag antibody F9291 was used and for dup$\Delta\alpha$7, an anti-his antibody from Abbexa Ltd was chosen. The last one did not work well and only showed some unspecific binding. Also, experiments with other anti-his antibodies did not work well. Therefore, the stainings of the dup$\Delta\alpha$7 need to be optimised and repeated.

4.5.3.1 α7N S1 antibody

HEK-293 cells were transfected with the human myc-tagged CHRNA7 subunits in combination with plasmids containing the DNA of the chaperons NACHO and RIC-3. The positive control with the anti-myc antibody 4A6 is shown in panels B and E of Figure 4.15. All cells stained with this antibody are transfected, have expressed the receptor and are expected to be recognised by the α7N antibody too (shown in Figure 4.15, panels A and D).

In addition, a comparison was made between cells treated with Triton X and Tween 20 and cells not treated with them. These reagents increase the membrane permeability of the cells and allow the antibody to bind intracellular epitopes as well. As the binding site of α7N S1 is at the N-terminus of the subunits, located extracellularly, it should show positive results without these reagents. With the comparison it is possible to determine whether the subunits form a receptor which is inserted into the plasma membrane or if those receptors are constrained to the cytoplasm.

The results show that both antibodies, positive control and α7N S1, bind equally to the protein. Also, it is to be assumed that the receptor is built into the membrane, otherwise there would be no staining visible in panels D-F.

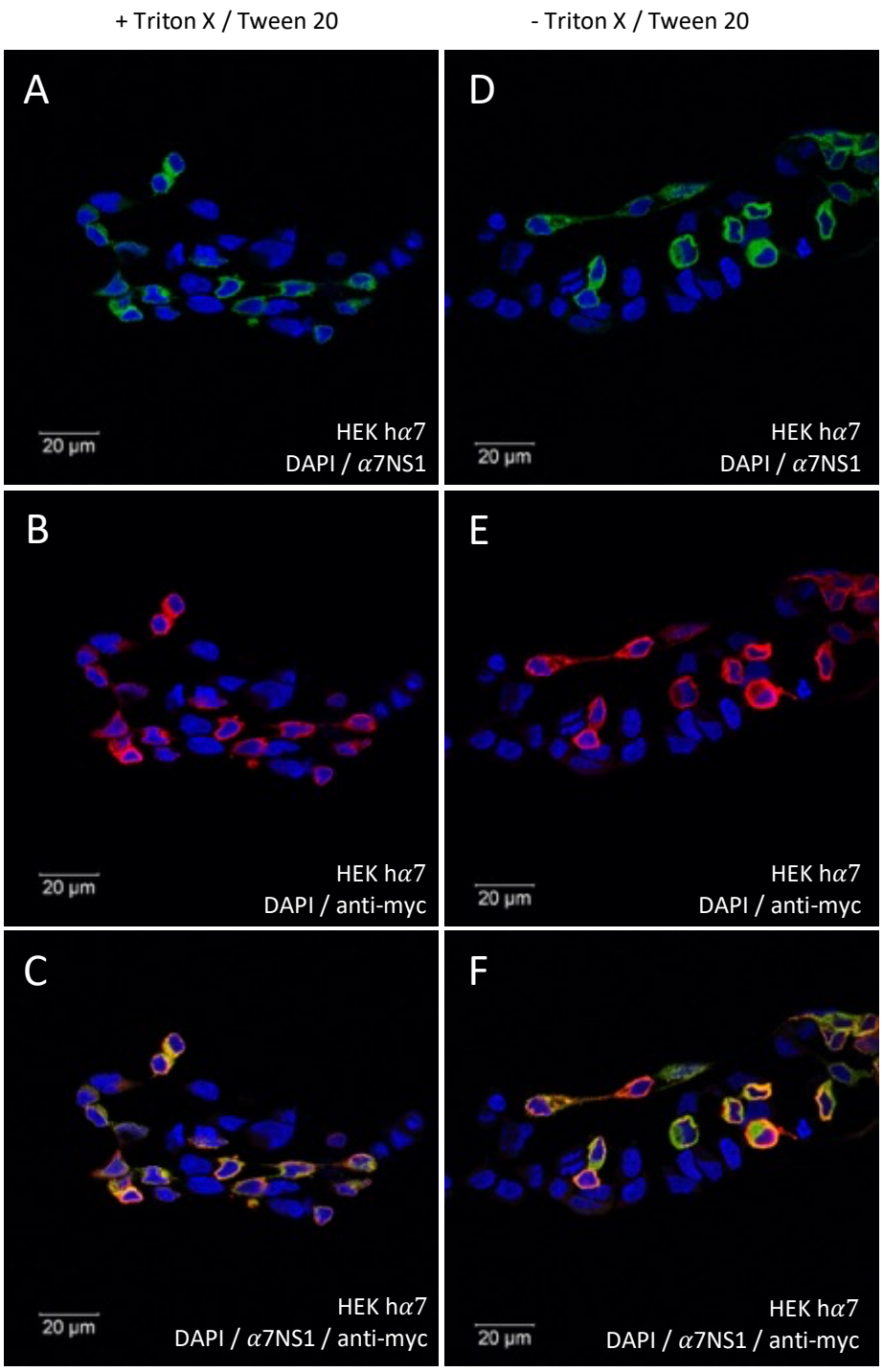

Figure 4.15: *HEK-293 cells transfected with plasmids containing the human myc-tagged CHRNA7, NACHO and RIC-3, stained with the antibody α7N S1.*
Panels A-C: Cells stained in presence of Triton X and Tween 20 with α7N S1 (panel A) and anti-myc 4A6 as positive control (panel B), overlay (panel C). Panels D-F: Cells stained in absence of Triton X and Tween 20 with α7N S1 (panel D) and anti-myc 4A6 as positive control (panel E), overlay (panel F).

4.5.3.2 α7L S3 and S4 antibody

The α7L antibodies were gained from rabbits immunised against the intracellular loop region of the subunits. This region is the same in the full length α7 subunit as well as in the dupα7 and dupΔα7 construct. Therefore, the α7L antibodies should detect all of the three proteins.

α7L S3 and S4 antibody on HEK cells transfected with CHRNA7

In Figure 4.16 the results of both antibodies, α7L S3 and S4, applied on HEK cells transfected with plasmids coding for CHRNA7 in addition with the chaperons NACHO and RIC-3, are shown. The α7L S3 antibody gave the most promising results (panels A-C). As expected, the cells stained with the positive control (panel B) are also stained with α7L S3 in a comparable intensity, shown in panel A.

The results for the second loop antibody, α7LS4, are shown in panels D-F. The positive control in panel E shows the transfected cells, stained with the anti-myc 4A6 antibody. There is no staining in green in panel D visible, which means that the α7LS4 antibody did not work in this experiment.

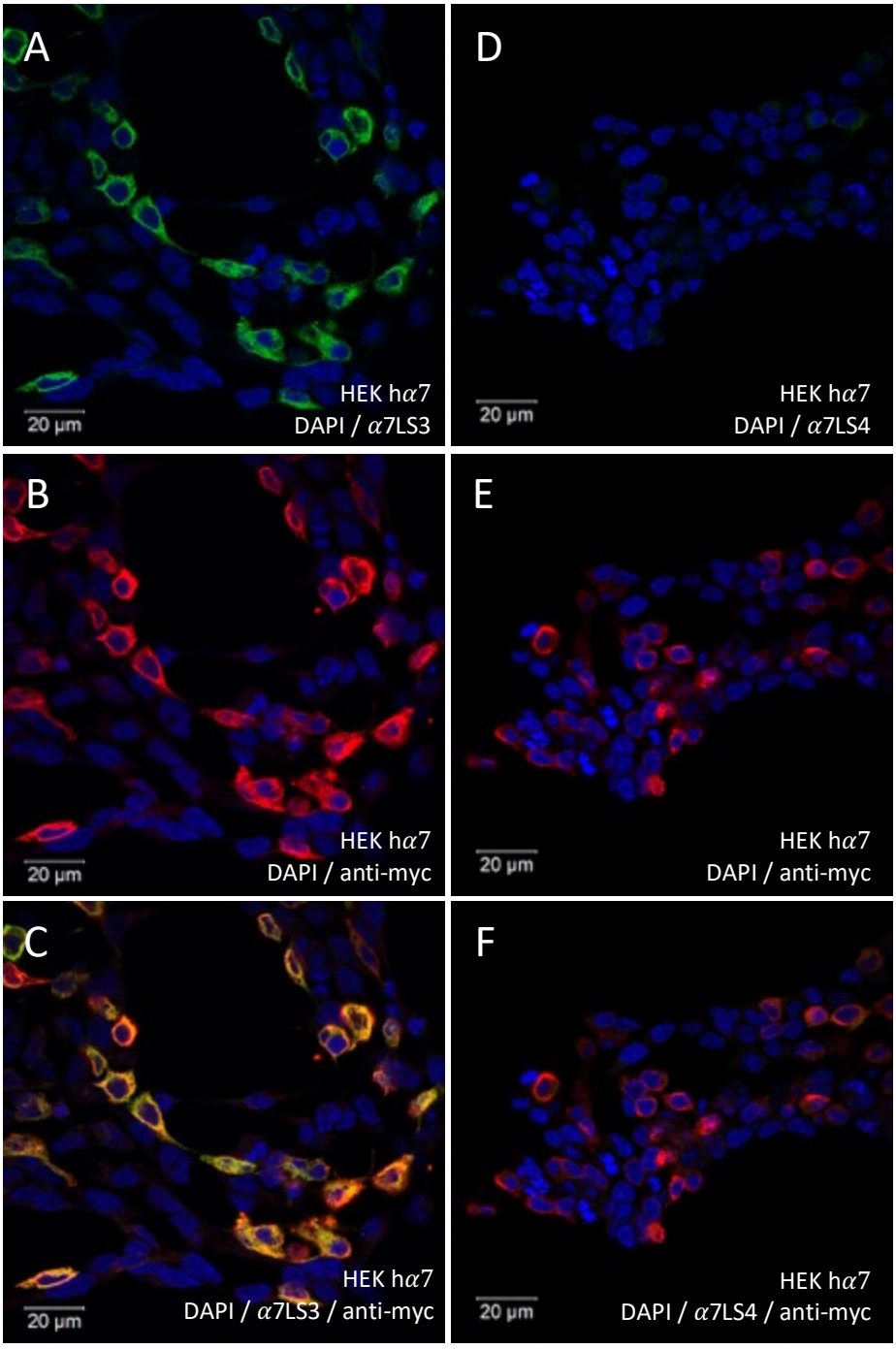

***Figure 4.16**: HEK-293 cells transfected with plasmids containing the human myc-tagged CHRNA7, NACHO and RIC-3, stained with the antibodies α7LS3 and S4.*
Panels A-C: Cells stained with α7LS3 (panel A) and anti-myc 4A6 as positive control (panel B), overlay (panel C).
Panels D-F: Cells stained with α7LS4 (panel D) and anti-myc 4A6 as positive control (panel E), overlay (panel F).

α7L S3 and S4 antibody on HEK cells transfected with CHRFAM7A

As previously mentioned, the α7L antibodies should also recognise the loop region of the duplicated subunits. Therefore, HEK cells were transfected with plasmids containing the DNA sequence of dupα7 and the chaperons NACHO and RIC-3. A comparison was made with cells which were additionally transfected with the human CHRNA7, since there is the hypothesis

that the duplicated subunits will not form a receptor on their own and need to co-assemble with α7 (see chapter 1.3.2). The results for α7L S3 are shown and compared in Figure 4.17. Panels A-C show HEK cells transfected with CHRFAM7A and panels D-F show them additionally transfected with CHRNA7. The cells with most intense staining at the positive control (panels B and E) are also stained by α7L S3. More cells are stained by the α7L antibody when CHRFAM7A is co-transfected with CHRNA7.

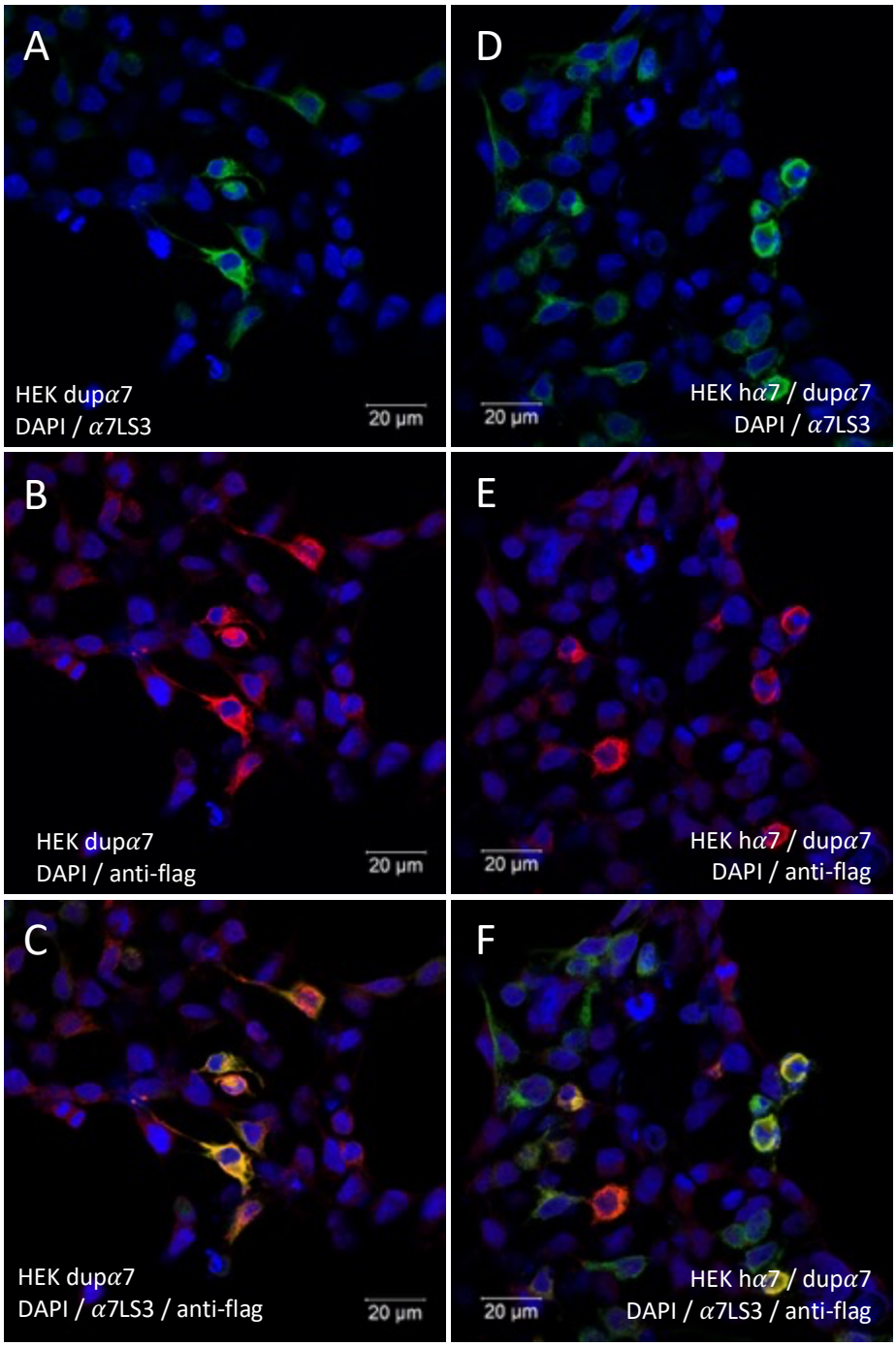

Figure 4.17: *A-C: HEK-293 cells transfected with plasmids containing the flag-tagged CHRFAM7A, NACHO and RIC-3; cells were stained with the antibody α7LS3.*
Panels A-C: Cells stained with α7LS3 (panel A) and anti-flag F9291 as positive control (panel B), overlay (panel C). Panels D-F: Cells transfected additionally with human myc-tagged CHRNA7, stained with α7LS3 (panel D) and anti-flag F9291 as positive control (panel E), overlay (panel F).

The staining with α7LS4 gave no clear results. Since in this experiment, the positive control with the anti-flag antibody stained not many cells and gave a very weak signal which indicates that the experiment failed and needs to be repeated.

α7L S3 and S4 antibody on HEK cells transfected with CHRFAM7AΔ2bp

Thirdly, the loop antibodies were tested on HEK cells transfected with CHRFAM7AΔ2bp and the chaperons. Like described before, some cells were additionally transfected with the full-length α7 subunit. An anti-his antibody from Abbexa Ltd was chosen as positive control.
In Figure 4.18 the results for α7LS3 are shown. In panels A and D, the tested antibody binds his target. Unfortunately, the his-staining in panels B and E only showed unspecific binding and background signals. Therefore, this anti-his-antibody seems not to be suitable as positive control. The experiment needs to be optimised and repeated, since the accuracy and correctness of the results cannot be guaranteed without the positive control.

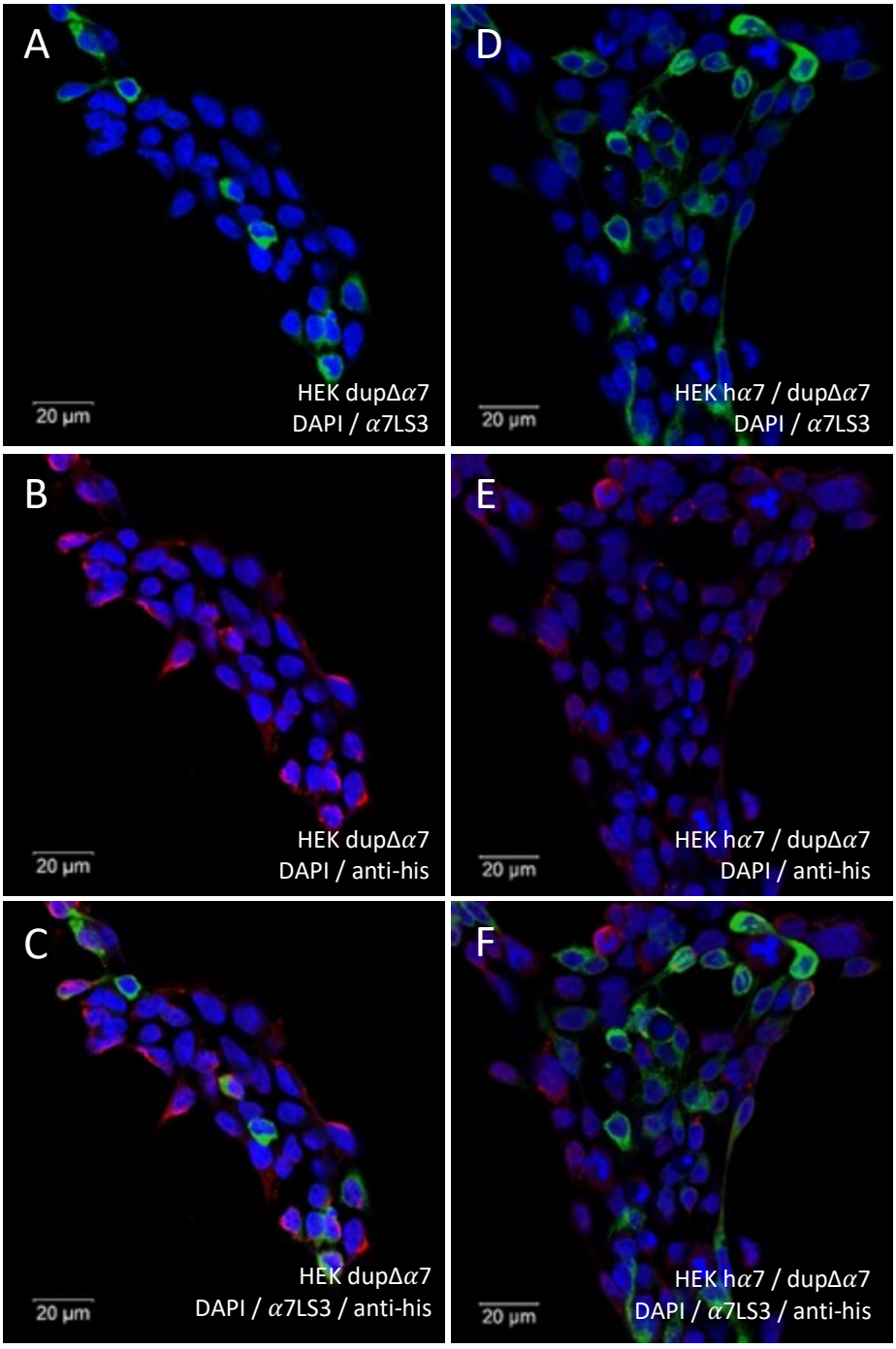

Figure 4.18: *A-C: HEK-293 cells transfected with plasmids containing his-tagged CHRFAM7AΔ2bp, NACHO and RIC-3; cells were stained with the antibody α7LS3.*
Panels A-C: Cells stained with α7L S3 (panel A) and anti-his (abbexa) as positive control (panel B), overlay (panel C). Panels D-F: Cells transfected additionally with myc-tagged CHRNA7, stained with α7LS3 (panel D) and anti-his (abbexa) as positive control (panel E), overlay (panel F).

For a similar experiment with the α7LS4 antibody, another anti-his antibody from the company Santa Cruz was chosen. This antibody was also gained from rabbits, which means that both antibodies needed to be tested on different cells, as both were detected with a secondary anti-rabbit antibody conjugated to Alexa Flour® 488. But the results also just

showed some unspecific binding at all conditions. Nearly no cells were stained and there was just some background signal visible.

4.5.3.3 Dupα7N S5 antibody

The dupα7N S5 antibody was tested under four conditions. On the one hand it was applied to HEK cells transfected with plasmids containing the flag-tagged CHRFAM7A and the chaperons NACHO and RIC-3. On the other hand, it was applied to cells additionally transfected with CHRNA7-plasmid. These two combinations were stained once in absence of Triton X and Tween 20 and once in presence of Triton X and Tween 20 since the antibodies should recognise a region at the extracellular N-terminus. The results of the cells treated with Triton X and Tween 20 and stained with dupα7N S5 are shown in Figure 4.19. Since the positive control showed good results, it was concluded that cells have been transfected and the expression of the construct was achieved. However, the dupα7N S5 antibody displayed no staining (panels A and D), therefore we conclude that this antibody is not suited for these types of experiments.

Cells without Triton X and Tween 20 treatment did not show any staining, except for the nuclear DAPI (Figure 4.19, panels D-F).

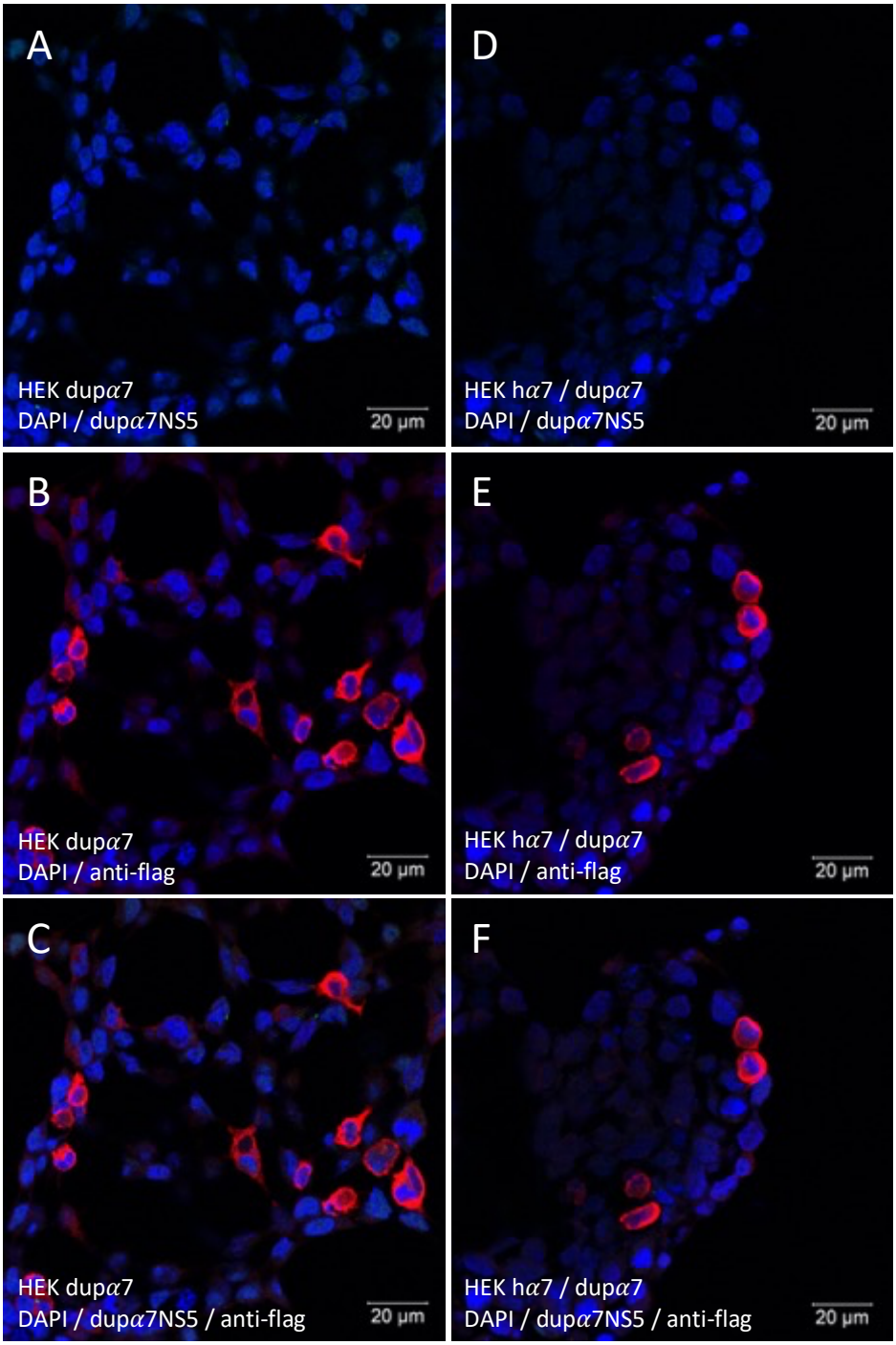

Figure 4.19: *A-C: HEK-293 cells transfected with plasmids containing flag-tagged CHRFAM7A, NACHO and RIC-3, stained with dupα7N S5.*
Panels A-C: cells stained with dupα7N S5 (panel A) and anti-flag F9291 as positive control (panel B), overlay (panel C). Panels D-F: Cells transfected additionally with myc-tagged CHRNA7, stained with dupα7N S5 (panel D) and anti-flag F9291 as positive control (panel E), overlay (panel F).

4.5.3.4 2bpα7N S7 antibody

Last, the 2bpα7N S7 antibody was tested. Like the dupα7N antibody, this one was also tested under four conditions. First on cells transfected with plasmids containing CHRFAM7AΔ2bp and the chaperons and second on cells co-transfected with CHRNA7-plasmid. A comparison

between cells treated with Triton X and Tween 20 or not was made again, since this antibody should also bind at the N-terminus of the subunit.

The 2bpα7N S7 antibody gave no immunocytochemical staining, but neither did the positive control. This time an anti-his antibody from Qiagen was used, but it also did not detect any proteins. Only some unspecific background signals were visible. Therefore, the anti-his staining needs to be optimised, and the experiments need to be repeated.

5 Discussion

The aim of this thesis was to characterise different antibodies in order to evaluate their suitability for certain methods in further studies. We analysed seven already established antibodies and a generation of new antibodies and the results were quite diverse.

To evaluate the quality of our antibodies, we performed western-blot and immunocytochemical experiments. First, we needed to choose an appropriate sample material. We chose rodent tissue from habenula and hippocampus as these are the brain regions with the largest amounts of the subunits examined [17,24]. Tissue from rodents is easily available, however when it comes to brain tissues from knockout mice, it becomes more limited. In our lab (among others) β2- and β4-knockout mice were accessible, however no α3- and α4-knockout animals. α3 knock-out mice display autonomic deficiency, have impaired growth and increased perinatal mortality [54] and can therefore not be bred easily. Thus, for our experiments concerning the α3 and α4 subunit, samples from β2- and β4-knockout animals were used. This is possible, since in the habenula, the α3 subunit preferentially co-assembles with β4. Therefore, the levels of α3 have been shown to be significantly decreased in β4-knockout tissue to less than 20% [53]. The same applies to α4 and β2, which co-assemble, and a deletion of β2 also leads to a significant reduction of α4 in habenula [53]. We therefore expect α3 signals to be significantly reduced in β4- and α4 signals in β2-knockout mouse tissue. However, since we were mostly interested in the nAChR subunits of the human brain, we also needed a representative alternative for human brain tissue. This is especially true for the analysis of the newly generated anti-α7 antibodies, since dupα7 and dup$\Delta\alpha$7 can only be found in humans (see chapter 1.3) [31]. Therefore, most of our experiments rely on transfected HEK cells. These provide many advantages as platform for the expression of receptor proteins. As mammalian cells, they are capable of expressing a variety of different proteins, ensuring post-translational processes such as folding or glycosylation. Another reason for using HEK cells is the high cell division rate and the possibility of harvesting the protein only a few days after transfection [55]. HEK-293 cells are thus a useful vehicle for the expression and the investigation of nACh receptors [56].

The already mentioned paper from Moser et al shows very well how important it is to characterise antibodies. In this study the suitability of commercially available antibodies,

which were presumed to be specific for the different nAChR subunits, was evaluated. Therefore, the antibodies were tested by five different laboratories with standard protocols for western blot and immunohistochemistry using brain lysates from wild type and knockout mice. In Figure 5.1 the results of some western blots are shown, and these are speaking against the specificity of the antibodies. In nearly all of them the visible bands are at the same height with the same intensity in wild type, as well as in knockout tissue. Additionally, not all bands are at the expected size for the subunit. For example, the α4 subunit has a prospected size of around 70kDa and the band was detected at about 100kDa. The bands for the α7 subunit were approximately at the correct height with around 48 and 52 instead of 56kDa, but there are signals for the knock-out tissue as well. Thus, results with currently available nAChR antibodies must be interpreted with caution [51].

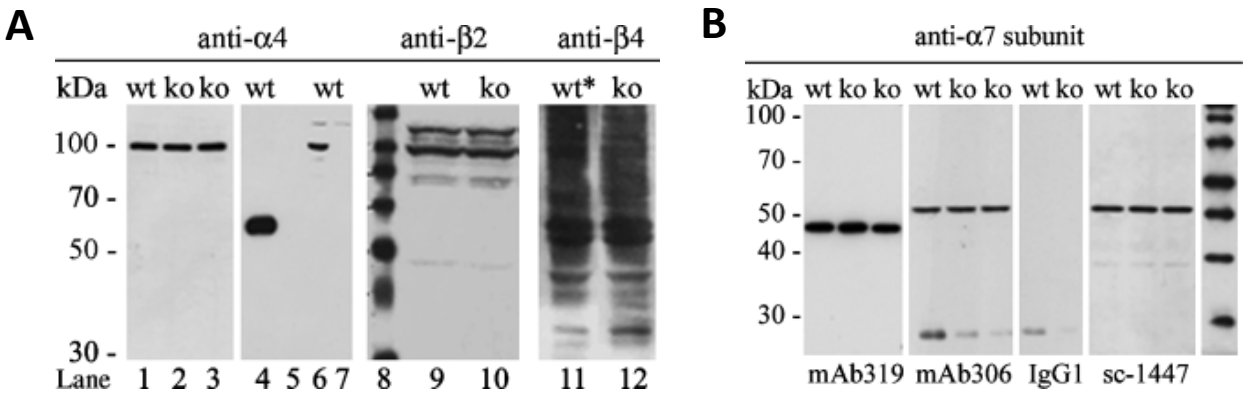

Figure 5.1: *Western Blots incubated with nAChR subunit specific antibodies using brain lysates of wt and ko mice* [51].
A. Brain lysates of wt and ko mice, detection with different antibodies against the α4-, β3 or β4-subunit B. 5 µg of wt or ko mice brain lysate per lane, detection with different anti-α7 antibodies

Our first set of experiments tested the quality of our antibodies in western blot experiments. As mentioned above, we focused on the specificity of our signals, and kept an eye on discovering unspecific bands. This problem, however, only occurred in a minor extent in our western blots. At one of them, the one incubated with the β4S4 antibody, an unspecific signal for knockout tissue has been detected. But this band was detected at a smaller size than the expected protein size for the β4 subunit and all of the other signals. The α7S26 antibody gave an unspecific signal for untransfected HEK cells, but this could also be a result of the applied concentration, since all of the other applied cell suspensions were diluted four times higher as these. All of the other antibodies showed good selectivity in western blot as they did not recognise any proteins in knockout tissue or untransfected HEK cells. All signals were observed at the correct size for each subunit.

However, in some of our western-blot experiments, an additional problem occurred. The signals for HEK cells, especially for those transfected with the mouse proteins, often did not give well-defined bands. The band at the correct height for the protein was clearly the most intense but above and below there were weaker additional bands. This problem occurred particularly with the blot incubated with the α7L S3 antibody. The lanes were heavily overloaded, consequently the picture was taken with just a few seconds of exposure time. The reason for that could be too high expression levels of α7, due to the pUNIV expression-vector that was used for transfection. The pUNIV-vector has been especially designed to yield high level, stable expression in multiple cell types [57] but possibly under our conditions the expression levels were higher than expected and the samples should have been diluted to a higher extent. This will be considered in future experiments. In addition, unfortunately, the α7 antibody did not recognise any of the proteins in rodent hippocampus. Possibly, especially compared to the transfected cells, α7-protein levels were below the detection limit in the native tissue. In future experiments the native tissue will have to be used at higher concentration and/or the receptors enriched by immunoprecipitation or alpha-bungarotoxin immunopurification. Summarizing in our western blot experiments, three antibodies could be identified, which can be used to detect human nAChR subunits: α3S1, β2S19 and α7L S3.

If the specificity and suitability of an antibody is demonstrated with certain methods, like western blot, the results can usually only be guaranteed for the specific method used. For the use in other techniques the suitability can't be assumed to be the same [58]. That is why we did not only analyse our antibodies by western blot, but also in ICC. For these experiments HEK cells were transfected with plasmids coding for proteins tagged with either a myc-, flag- or his-tag. The α7-subunit was tagged with a myc-tag, the dupα7 with a flag-tag and the dup$\Delta\alpha$7 with a his-tag. This gives the unique advantage, that we can detect the transfected cells with a well characterized, commercially available antibody as reference. This strategy worked well for the myc- and the flag-tagged constructs. For the third his-tagged protein additional experiments are required.

Indeed, we were able to identify two independent antibodies, which are suitable for the ICC-technique: α7N S1, which is specific for α7 only and α7L S3, which can detect all three α7-nAChR-subunit isoforms.

5.1 Conclusions and outlook

5.1.1 Summary for α3, α4, β2 and β4

Since the amino acid alignments of the α3 and β2 subunit gave an identity of 84.5% for the α3 subunit and 76.1% for the β2 subunit, we expected that the antibodies against these subunits are able to recognise the human subunits in western blot as well as in immunocytochemistry. These predictions were confirmed and α3S1 as well as β2S19 gave the expected results in both methods.

The amino acid sequences of the rodent and human β4 subunits only have an identity of 44.0% and the antibodies against it do not recognise the human subunit. We tested four different antibodies, from which β4S5 gave the best results in both methods, western blot and ICC. In western blot experiments the other antibodies, β4S4, β4S6 and β4S22, only detected the mouse subunit in transfected HEK cells, except for β4S4 which gave some signal in wild type mouse and rat brain tissue, but also some unspecific signal for knockout tissue. Therefore, all three antibodies are not suitable for our purpose and were not further characterised with ICC.

The expectations that the α4S26 antibody would recognise the α4 subunit from human were not high, since the amino acid alignments only showed an identity of 53.7%. In western blot these expectations proved true and further ICC experiments were therefore not performed.

5.1.1 Summary for anti- α7 antibodies

The new generation of anti-α7 antibodies was characterised with two experimental methods, western blot and immunocytochemistry. In western blot the α7L S3 antibody seems to give promising results, but there is definitely an optimisation needed, because of the aspects mentioned above.

In the immunocytochemical experiments the α7NS1 antibody and the α7LS3 antibody gave promising results. Both stained the cells comparably to our positive control. All other antibodies gave no staining or in case of the dupα7N S5 antibody the positive control did not work, and the experiment needs to be revised and repeated.

5.1.2 Outlook

For the new generation of α7 antibodies a further investigation and characterisation definitely needs to be done. First, the already mentioned optimisation of the western blots with the new

generation of the anti-α7 antibodies and a further investigation of the positive control with the his-tag in ICC would be an important issue. The question coming up here is whether the anti-his antibody is not suitable for this experiment or if there is a problem with the dup$\Delta\alpha$7-construct.

In addition, so far, we have only analysed the antibodies isolated from the first blood samples, gained after the third immunisation of the rabbits. As soon as further antibodies are purified from blood draws taken later, these also need to be characterised and the results might be different, since there was the fourth immunisation of the rabbits in between.

Furthermore, not all antibodies were tested in ICC yet. With the dupα7N S6 and the 2bpα7N S8 antibodies, no ICC experiments were performed yet.

Last, a characterisation with immunohistochemistry was also planned and the first experiments to find the right materials and methods have already been started. However, there are no presentable results yet.

6 Copyright Statement

I have tried to locate all copyright owners to obtain permission for reusing their content in this thesis. Should any copyright infringement become known, please contact me immediately.

Figure 1.1: Structure of nAChRs [11]. Reused with permission from www.copyright.com; License Number: 5039371080769, License Date: Mar 31, 2021

Figure 1.2: Duplication of the CHRNA7 gene [32]. Reused with permission from www.copyright.com; License Number: 5038951199712, License Date: Mar 30, 2021

Figure 1.3: Translation products of CHFAM7A and CHRFAM7AΔ2bp [32]. Reused with permission from www.copyright.com; License Number: 5038951199712, License Date: Mar 30, 2021

Figure 1.4: Topology of CHRNA7, CHRFAM7A and CHRFAM7AΔ2bp gene products [32]. Reused with permission from www.copyright.com; License Number: 5038951199712, License Date: Mar 30, 2021

Figure 5.1: Western Blots incubated with nAChR subunit specific antibodies using brain lysates of wt and ko mice [51]. Reused with permission from www.copyright.com; License Number: 5039220954018, License Date: Mar 31, 2021

7 References

[1] Gotti, C. and Clementi, F. (2004) Neuronal nicotinic receptors: From structure to pathology. *Progress in Neurobiology*. 74 (6), 363–396.

[2] Albuquerque, E.X., Pereira, E.F.R., Alkondon, M., and Rogers, S.W. (2009) Mammalian nicotinic acetylcholine receptors: From structure to function. *Physiological Reviews*. 89 (1), 73–120.

[3] Hogg, R.C., Raggenbass, M., and Bertrand, D. (2003) Nicotinic acetylcholine receptors: from structure to brain function. in: Rev. Physiol. Biochem. Pharmacol., Springer Berlin Heidelberg, Berlin, Heidelbergpp. 1–46.

[4] Dani, J.A. and Bertrand, D. (2007) Nicotinic acetylcholine receptors and nicotinic cholinergic mechanisms of the central nervous system. *Annual Review of Pharmacology and Toxicology*. 47 699–729.

[5] Wessler, I., Kilbinger, H., Bittinger, F., Unger, R., and Kirkpatrick, C.J. (2003) The non-neuronal cholinergic system in humans: Expression, function and pathophysiology. *Life Sciences*. 72 (18–19), 2055–2061.

[6] Jensen, A.A., Frølund, B., Liljefors, T., and Krogsgaard-Larsen, P. (2005) Neuronal nicotinic acetylcholine receptors: Structural revelations, target identifications, and therapeutic inspirations. *Journal of Medicinal Chemistry*. 48 (15), 4705–4745.

[7] Unwin, N. (2005) Refined structure of the nicotinic acetylcholine receptor at 4 Å resolution. *Journal of Molecular Biology*. 346 (4), 967–989.

[8] Gotti, C., Clementi, F., Fornari, A., Gaimarri, A., Guiducci, S., Manfredi, I., et al. (2009) Structural and functional diversity of native brain neuronal nicotinic receptors. *Biochemical Pharmacology*. 78 (7), 703–711.

[9] McKay, B.E., Placzek, A.N., and Dani, J.A. (2007) Regulation of synaptic transmission and plasticity by neuronal nicotinic acetylcholine receptors. *Biochemical Pharmacology*. 74 (8), 1120–1133.

[10] Nys, M., Kesters, D., and Ulens, C. (2013) Structural insights into Cys-loop receptor function and ligand recognition. *Biochemical Pharmacology*. 86 (8), 1042–1053.

[11] Changeux, J.P. (2010) Nicotine addiction and nicotinic receptors: Lessons from genetically modified mice. *Nature Reviews Neuroscience*. 11 (6), 389–401.

[12] Miyazawa, A., Fujiyoshi, Y., and Unwin, N. (2003) Structure and gating mechanism of the acetylcholine receptor pore. *Nature*. 423 (6943), 949–955.

[13] Keramidas, A., Moorhouse, A.J., Schofield, P.R., and Barry, P.H. (2004) Ligand-gated ion channels: Mechanisms underlying ion selectivity. *Progress in Biophysics and Molecular Biology*. 86 (2), 161–204.

[14] Gotti, C., Zoli, M., and Clementi, F. (2006) Brain nicotinic acetylcholine receptors: native subtypes and their relevance. *Trends in Pharmacological Sciences*. 27 (9), 482–491.

[15] Pierre-Jean Corringer, N.L.N. and Changeux, and J.-P. (2000) Nicotinic Receptors at the Amino Acid Level. *Annual Review of Pharmacology and Toxicology*. 40 431–58.

[16] Picciotto, M.R., Caldarone, B.J., Brunzell, D.H., Zachariou, V., Stevens, T.R., and King, S.L. (2001) Neuronal nicotinic acetylcholine receptor subunit knockout mice: Physiological and behavioral phenotypes and possible clinical implications. *Pharmacology and Therapeutics*. 92 (2–3), 89–108.

[17] Gotti, C., Moretti, M., Gaimarri, A., Zanardi, A., Clementi, F., and Zoli, M. (2007) Heterogeneity and complexity of native brain nicotinic receptors. *Biochemical*

Pharmacology. 74 (8), 1102–11.
[18] Lindstrom, J. (1997) Nicotinic acetylcholine receptors in health and disease. *Molecular Neurobiology*. 15 (2), 193–222.
[19] Buisson, B. and Bertrand, D. (2002) Nicotine addiction: The possible role of functional upregulation. *Trends in Pharmacological Sciences*. 23 (3), 130–136.
[20] Gotti, C., Moretti, M., Bohr, I., Ziabreva, I., Vailati, S., Longhi, R., et al. (2006) Selective nicotinic acetylcholine receptor subunit deficits identified in Alzheimer's disease, Parkinson's disease and dementia with Lewy bodies by immunoprecipitation. *Neurobiology of Disease*. 23 (2), 481–489.
[21] Cordero-Erausquin, M., Marubio, L.M., Klink, R., and Changeux, J.P. (2000) Nicotinic receptor function: New perspectives from knockout mice. *Trends in Pharmacological Sciences*. 21 (6), 211–217.
[22] Bina, K.G., Guzman, P., Broide, R.S., Leslie, F.M., Smith, M.A., and O'Dowd, D.K. (1995) Localization of α7 nicotinic receptor subunit mRNA and α-bungarotoxin binding sites in developing mouse somatosensory thalamocortical system. *Journal of Comparative Neurology*. 363 (2), 321–332.
[23] De Jonge, W.J. and Ulloa, L. (2007) The alpha7 nicotinic acetylcholine receptor as a pharmacological target for inflammation. *British Journal of Pharmacology*. 151 (7), 915–929.
[24] Orr-Urtreger, A., Göldner, F.M., Saeki, M., Lorenzo, I., Goldberg, L., De Biasi, M., et al. (1997) Mice deficient in the neuronal nicotinic acetylcholine receptor lack α-bungarotoxin binding sites and hippocampal fast nicotinic currents. *Journal of Neuroscience*. 17 (23), 9165–9171.
[25] Le Novère, N., Corringer, P.J., and Changeux, J.P. (2002) The diversity of subunit composition in nAChRs: Evolutionary origins, physiologic and pharmacologic consequences. *Journal of Neurobiology*. 53 (4), 447–456.
[26] Hurst, R., Rollema, H., and Bertrand, D. (2013) Nicotinic acetylcholine receptors: From basic science to therapeutics. *Pharmacology and Therapeutics*. 137 (1), 22–54.
[27] Freedman, R., Coon, H., Myles-Worsley, M., Orr-Urtreger, A., Olincy, A., Davis, A., et al. (1997) Linkage of a neurophysiological deficit in schizophrenia to a chromosome 15 locus. *Proceedings of the National Academy of Sciences of the United States of America*. 94 (2), 587–592.
[28] Gault, J., Robinson, M., Berger, R., Drebing, C., Logel, J., Hopkins, J., et al. (1998) Genomic organization and partial duplication of the human α7 neuronal nicotinic acetylcholine receptor gene (CHRNA7). *Genomics*. 52 (2), 173–185.
[29] De Lucas-Cerrillo, A.M., Maldifassi, M.C., Arnalich, F., Renart, J., Atienza, G., Serantes, R., et al. (2011) Function of partially duplicated human α7 nicotinic receptor subunit CHRFAM7A gene: Potential implications for the cholinergic anti-inflammatory response. *Journal of Biological Chemistry*. 286 (1), 594–606.
[30] Stephens, S.H., Logel, J., Barton, A., Franks, A., Schultz, J., Short, M., et al. (2009) Association of the 5'-upstream regulatory region of the α7 nicotinic acetylcholine receptor subunit gene (CHRNA7) with schizophrenia. *Schizophrenia Research*. 109 (1–3), 102–112.
[31] Dennis, M.Y., Harshman, L., Nelson, B.J., Penn, O., Cantsilieris, S., Huddleston, J., et al. (2017) The evolution and population diversity of human-specific segmental duplications. *Nature Ecology and Evolution*. 1 (3), 1–10.
[32] Sinkus, M.L., Graw, S., Freedman, R., Ross, R.G., Lester, H.A., and Leonard, S. (2015) The human CHRNA7 and CHRFAM7A genes: A review of the genetics, regulation, and

function. *Neuropharmacology*. 96 (PB), 274–288.
[33] Riley, B., Williamson, M., Collier, D., Wilkie, H., and Makoff, A. (2002) A 3-Mb map of a large segmental duplication overlapping the α7-nicotinic acetylcholine receptor gene (CHRNA7) at human 15q13-q14. *Genomics*. 79 (2), 197–209.
[34] Flomen, R.H., Davies, A.F., Di Forti, M., La Cascia, C., Mackie-Ogilvie, C., Murray, R., et al. (2008) The copy number variant involving part of the α7 nicotinic receptor gene contains a polymorphic inversion. *European Journal of Human Genetics*. 16 (11), 1364–1371.
[35] Sinkus, M.L., Lee, M.J., Gault, J., Logel, J., Short, M., Freedman, R., et al. (2009) A 2-base pair deletion polymorphism in the partial duplication of the α7 nicotinic acetylcholine gene (CHRFAM7A) on chromosome 15q14 is associated with schizophrenia. *Brain Research*. 1291 1–11.
[36] Wang, Y., Xiao, C., Indersmitten, T., Freedman, R., Leonard, S., and Lester, H.A. (2014) The duplicated α7 subunits assemble and form functional nicotinic receptors with the full-length α7. *Journal of Biological Chemistry*. 289 (38), 26451–26463.
[37] Araud, T., Graw, S., Berger, R., Lee, M., Neveu, E., Bertrand, D., et al. (2011) The chimeric gene CHRFAM7A, a partial duplication of the CHRNA7 gene, is a dominant negative regulator of α7*nAChR function. *Biochemical Pharmacology*. 82 (8), 904–914.
[38] Chan, T., Williams, E., Cohen, O., Eliceiri, B.P., Baird, A., and Costantini, T.W. (2019) CHRFAM7A alters binding to the neuronal alpha-7 nicotinic acetylcholine receptor. *Neuroscience Letters*. 690 126–131.
[39] Halevi, S., Yassin, L., Eshel, M., Sala, F., Sala, S., Criado, M., et al. (2003) Conservation within the RIC-3 gene family: Effectors of mammalian nicotinic acetylcholine receptor expression. *Journal of Biological Chemistry*. 278 (36), 34411–34417.
[40] Millar, N.S. (2008) RIC-3: A nicotinic acetylcholine receptor chaperone. *British Journal of Pharmacology*. 153 (SUPPL. 1), 177–183.
[41] Gu, S., Matta, J.A., Lord, B., Harrington, A.W., Sutton, S.W., Davini, W.B., et al. (2016) Brain α7 Nicotinic Acetylcholine Receptor Assembly Requires NACHO. *Neuron*. 89 (5), 948–955.
[42] Matta, J.A., Gu, S., Davini, W.B., Lord, B., Siuda, E.R., Harrington, A.W., et al. (2017) NACHO Mediates Nicotinic Acetylcholine Receptor Function throughout the Brain. *Cell Reports*. 19 (4), 688–696.
[43] Kouvatsos, N., Giastas, P., Chroni-Tzartou, D., Poulopoulou, C., and Tzartos, S.J. (2016) Crystal structure of a human neuronal nAChR extracellular domain in pentameric assembly: Ligand-bound α2 homopentamer. *Proceedings of the National Academy of Sciences of the United States of America*. 113 (34), 9635–9640.
[44] Nguyen, M., Alfonso, A., Johnson, C.D., and Rand, J.B. (1995) Caenorhabditis elegans mutants resistant to inhibitors of acetylcholinesterase. *Genetics*. 140 (2), 527–535.
[45] Castelán, F., Castillo, M., Mulet, J., Sala, S., Sala, F., Domínguez Del Toro, E., et al. (2008) Molecular characterization and localization of the RIC-3 protein, an effector of nicotinic acetylcholine receptor expression. *Journal of Neurochemistry*. 105 (3), 617–627.
[46] Mossier, B., Togel, M., Fuchs, K., and Siegharts, W. (1994) Immunoaffinity purification of gamma-aminobutyric acidA (GABAA) receptors containing gamma 1-subunits. *Journal of Biological Chemistry*. 269 (41), 25777–25782.
[47] David, R., Ciuraszkiewicz, A., Simeone, X., Orr-Urtreger, A., Papke, R.L., McIntosh, J.M., et al. (2010) Biochemical and functional properties of distinct nicotinic acetylcholine receptors in the superior cervical ganglion of mice with targeted deletions of nAChR subunit genes. *European Journal of Neuroscience*. 31 (6), 978–993.

[48] Koussounadis, A., Langdon, S.P., Um, I.H., Harrison, D.J., and Smith, V.A. (2015) Relationship between differentially expressed mRNA and mRNA-protein correlations in a xenograft model system. *Scientific Reports*. 5 10775.

[49] Mousavi, M., Hellström-Lindahl, E., Guan, Z.Z., Shan, K.R., Ravid, R., and Nordberg, A. (2003) Protein and mRNA levels of nicotinic receptors in brain of tobacco using controls and patients with Alzheimer's disease. *Neuroscience*. 122 (2), 515–520.

[50] Costantini, T.W., Chan, T.W., Cohen, O., Langness, S., Treadwell, S., Williams, E., et al. (2019) Uniquely human CHRFAM7A gene increases the hematopoietic stem cell reservoir in mice and amplifies their inflammatory response. *Proceedings of the National Academy of Sciences of the United States of America*. 116 (16), 7932–7940.

[51] Moser, N., Mechawar, N., Jones, I., Gochberg-Sarver, A., Orr-Urtreger, A., Plomann, M., et al. (2007) Evaluating the suitability of nicotinic acetylcholine receptor antibodies for standard immunodetection procedures. *Journal of Neurochemistry*. 102 (2), 479–492.

[52] Garg, B.K. and Loring, R.H. (2017) Evaluating Commercially Available Antibodies for Rat α7 Nicotinic Acetylcholine Receptors. *Journal of Histochemistry and Cytochemistry*. 65 (9), 499–512.

[53] Scholze, P., Koth, G., Orr-Urtreger, A., and Huck, S. (2012) Subunit composition of α5-containing nicotinic receptors in the rodent habenula. *Journal of Neurochemistry*. 121 (4), 551–560.

[54] Xu, W., Gelber, S., Orr-Urtreger, A., Armstrong, D., Lewis, R.A., Ou, C.N., et al. (1999) Megacystis, mydriasis, and ion channel defect in mice lacking the α3 neuronal nicotinic acetylcholine receptor. *Proceedings of the National Academy of Sciences of the United States of America*. 96 (10), 5746–5751.

[55] Thomas, P. and Smart, T.G. (2005) HEK293 cell line: A vehicle for the expression of recombinant proteins. *Journal of Pharmacological and Toxicological Methods*. 51 (3 SPEC. ISS.), 187–200.

[56] Xiao, Y. and Kellar, K.J. (2004) The comparative pharmacology and up-regulation of rat neuronal nicotinic receptor subtype binding sites stably expressed in transfected mammalian cells. *Journal of Pharmacology and Experimental Therapeutics*. 310 (1), 98–107.

[57] Venkatachalan, S.P., Bushman, J.D., Mercado, J.L., Sancar, F., Christopherson, K.R., and Boileau, A.J. (2007) Optimized expression vector for ion channel studies in Xenopus oocytes and mammalian cells using alfalfa mosaic virus. *Pflugers Archiv European Journal of Physiology*. 454 (1), 155–163.

[58] Bordeaux, J., Welsh, A.W., Agarwal, S., Killiam, E., Baquero, M.T., Hanna, J.A., et al. (2010) Antibody validation. *BioTechniques*. 48 (3), 197–209.

8 Appendix

8.1 List of Figures

8.2 List of Tables